Magnus Jervan

Parameter Identification for Adaptive Control of Autonomous Passenger Ferry

TTK4551 Specialization Project

Trondheim, December 2019

NTNU - Norwegian University of Science and Technology
Faculty of Information Technology and Electrical Engineering (IE)
Department of Engineering Cybernetics

Institutt for teknisk kybernetikk

Summary

In this thesis the goal is to identify the parameters of a ferry model. The ferry will be subject to a various numbers of passengers, which causes changes in the dynamics that can lead to less accurate control of the ferry. A model of the ferry is implemented into the controllers to give an output to the thrusters. When large deviations between the model and the actual dynamics of the system occurs, the accuracy of the controllers will decrease. It is tested through simulations if it is beneficial to identify these model changes, and give updated parameters to the controllers.

Four different parameter estimation methods are presented, and tested against each other in this thesis. The model of the ferry is complex with coupling terms between the states and nonlinear terms. The nonlinear parameters are kept constant, and the inertial matrix and the linear part of the damping matrix are identified. Two identification model are used. The simplest method only gives estimates of the diagonal parameters in the matrices, while keeping the coupling terms constant. This method is compared with an iterative method that is able to estimate all the parameters of the linear matrices, also the coupling terms. The parameter estimation is tested under ideal circumstances with persistent excitation of the input signal, and with simulated conditions representing driving under nominal operation. Under both conditions the parameters converged to the model value.
The simplest identification model has quicker convergence rate, as it does not have the complexity of estimating the coupling terms. This comes at the cost of the accuracy in the estimated model. With estimation of the coupling terms the convergence time is increased substantially, but all parameters do converge.

The parameter estimation methods are used to update the model in the controllers, and create a indirect adaptive controller. The distance and heading error between the ferry and the reference signal is measured to test the performance. This shows that all of the controllers benefits from an updated model. The discrepancies in the model from the simplest estimation method proved to be insignificant, and the increased complexity of estimating the coupling terms helped the performance of the controllers very little.

Preface

This thesis sums up the work of my specialization project at the Department of Engineering Cybernetics, NTNU. The thesis is carried out during the autumn semester of 2019 as part of the course TTK 4551 counting for 7.5 points. The project builds on the previous work on the autonomous ferry milliAmpere, with the aim of testing the possibility of an online system identification and implementation of an indirect adaptive control.

I would like to thank my supervisors Bjørn-Olav Holtung Eriksen and Morten Breivik for guidance sessions and valuable insight during this project.

Magnus Jervan
December 16, 2019
Trondheim, Norway

Table of Contents

List of Tables

List of Figures

Abbreviations

ABC Adaptive backstepping controller. viii, 4, 10, 11, 37, 42–47

DOF Degrees of freedom. 7, 21

IAE Integral Absolute Error. iii, vii, viii, 17, 37–39, 41–47

IMU Inertia measurement unit. 4

LOS Line of sight. iii, 11, 12, 19, 20, 32

LS Least-squares. 16, 25, 26, 30, 31, 33, 37, 39, 43–47

LSwFF Least-squares with forgetting factor. 16, 31, 33, 39, 43, 45, 46

MIMO Multiple input multiple output. 16

NED North-East-Down. 7, 8

PDwAFF PD with adaptive feedforward. iv, vii, viii, 4, 11, 37, 39–42, 45–47

PE Persistent excitation. vii, 13, 15, 16, 19, 21–24, 26, 27, 29, 31–33, 44, 45

PIDwFF PID with feedforward. iv, vii, 4, 10, 37–39, 41, 45–47

Chapter 1

Introduction

1.1 Motivation

Autonomous solutions are being developed on many platforms, both for vehicles on land and in the waters. Automated routes can be very beneficial as it can optimize transportation and free human resources from needing to operate a specific vehicle. By taking advantage of autonomous solutions, humans can supervise multiple automated vehicles at once rather than operating a single vehicle. With humans only needed when a vehicles can not solve the situation it self, and with every new situation an automated solution could be designed for the next time. This is why the marked is growing massively and new problems are solved every day.

Implementation of autonomous ferrys can help transportation by taking advantage of the water ways. They could take some of the burden of existing trafficated roads or be an alternative to building new bridges and tunnels. There are several places where crossing waters like rivers and canals is needed and this could be done with a low-cost autonomous ferry. It is a high construction and maintenance cost associated with creating tunnels or bridges, as well as the environmental cost from disturbing the natural environment with permanent structures. Autonomous electrically-powered ferries can serve as a more cost efficient solution. This could be transportation of vehicles, but also urban transport of pedestrians or bikers, which can make it more efficient and attractive to walk or use bicycles instead of cars.

For a self-driving vehicle to become fully automated without the need of supervision is unrealistic to this date, as there is so many unforeseen situations that it needs to handle. A group of automotive engineers from SAE International created what became the standard for evaluating the level of autonomy (SAEinternational, 2016). The different autonomy levels shown in Figure 1.1, gives a good perspective of the challenges designing a self-driving vehicle.

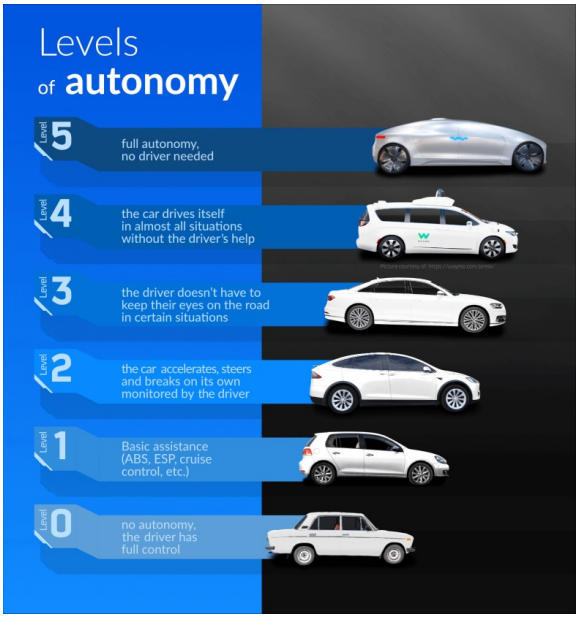

Figure 1.1: Five level of autonomy for self-driving vehicles, (OPONEO.CO.UK, 2016)

The same levels of autonomy could be compared with the ferry. To start with an autonomy of level 3 would be good, where it does most of the steering by its self, with someone at the controls ready to take over. To reach level 4 it would take a big step. It should handle all conditions that it operates in, and when transporting people the cost of faults is very high. The last level of autonomy is probably far away yet. This requires both the system, as well as the technology for the engine to be flawless. The trust in the equipment used should be immense, and engine stops or other system failures should be impossible. This makes a fully autonomous self-driving vehicle very hard to create.

To achieve an autonomous operating ferry where the goal is for humans only to monitor the operations, the system must be secure and trustworthy. Aiming to reach a autonomous system of level 3 on the ferry, it must be robust to handle all kinds of disturbances and changes that can occur. A model of the autonomous ferry is shown in Figure 1.2. different number of passengers will give a variation in load and weather conditions may change significantly with strong wind or large waves. This can change the dynamics of the ship and must be accounted for.

Figure 1.2: Model of the autonomous ferry, (Pedersen, 2019)

The plan is to install an autonomous ferry for urban transport in Trondheim, which will transport passengers from Ravnkloa across Nidelva to Vestre Kanalkai, as shown in Figure 1.3. The ferry should be able to transport 12 people at a time, and is ”on-demand”, making it ready to use when someone needs transportation. Now the work is done on a experimental ferry, milliAmpere, where the technology is being tested and developed for use on the autonomous ferry. The previous work done with this platform is described in section 1.2.

Figure 1.3: Planned route for autonomous ferry, (Pedersen, 2019)

1.2 Related work

In a previous masters thesis it was made a very precise model of milliAmpere by using optimization based system identification, (Pedersen, 2019). This method collects data on beforehand, and analyses the batch instead of an online system identification. An optimization problem is used to find the parameters in the model that gives the smallest quadratic error from the measurements. When comparing the model parameters to actual behaviour there are small deviations which indicates discrepancies in the model that is found. In this thesis the model parameters will be altered to simulate different mass in the tests. The parameters done from batch identification is done with an unspecified number of passengers, under good weather conditions with small wind gusts occasionally. It will arise changes in the dynamics of the ferry when passenger numbers and weather change. This could make it beneficial to update the parameters, resulting in more accurate estimates for the controller. An alternative could be to have different stationary models depending on number of passengers.

It is designed controllers able to steer the autonomous ferry to the desired position, in (Sæther, 2019), where a few different controllers for the ferry was tested. In simulations it was done tests with a PIDwFF, PDwAFF and a ABC. The ABC explained in subsection 2.2.2 uses a backstepping approach, and was the most accurate controller in the simulations, but with excessive actuator usage. The simulation model did not account for the time delay and slow dynamics of the thrusters, so when testing on the ferry the ABC was to aggressive and not applicable. The PDwAFF, derived in subsection 2.2.3, gave slightly better performance than regular feedforward, without to much extra actuator use. By designing a more robust ABC this could be made to fit with the actuators on the ferry. This could be compared with the other controllers together with an online system identification for the most accurate and robust system.

System identification of ships has been done in different ways before. Optimization techniques like using a support vector regression algorithm to find model parameters from zig-zag maneuvering test of ships (Zhu, 2019). This does not give online system identification, as the identification process must be done afterwards. As it is not online identification, changes in the dynamics will not be accounted for in the model. To deal with nonlinear ship models, the use of neural networks for system identification online is tested (Zheng, 2019). With learning algorithms it is needed computational power to process the data. There are few who have looked at model changes due to differences in load/passengers. Estimation of a ships mass is done with IMU based online estimation (Jonas Linder, 2015). This method uses a roll-model and is done to investigate the roll dynamics. If the mass could be estimated, the number of passengers would not necessarily be needed as it is the weight that effects the model. In the ship model of milliAmpere the roll dynamics are neglected, and therefore this is difficult to accomplish.

1.3 Problem description

In this thesis, the objective is to simulate the ferry with different loads and estimate the changes in the parameters. The parameter changes due to the changed dynamics is simulated to determine if the differences are significant. This will be used to investigate if it is beneficial with an online identification system and adaptive control to compensate for the changes.

It is tested if the changes in the dynamics is possible to estimate online, and if the performance is increased if updated parameters is used in the controllers.

The problem formulation is summarized in the following points:

- Perform a literature study of online system identification methods
- Design and evaluate the performance of online system identification methods
- Compare the performance of traditional feedback controllers with indirect adaptive controllers in simulations

1.4 Contributions

The ferry model is used to determine which parameters to identify. As the model is complex with coupling between the states and non linear terms, it is tested how this influences the parameter estimations. A method for identifying the coupling terms of the model matrices is derived and compared to a simpler method of ignoring them and keeping them constant. Different online parameter identification methods are implemented and tested through simulations. The estimation methods are evaluated by their convergence time when identifying the real values of the model, and large deviations as they are estimated. It is estimated how different number of passengers influence the ferry model and with these changes the existing controllers are compared to the controllers with estimation of the parameter changes.

1.5 Outline

This thesis is organized with the following chapters: Chapter 2 presents the theory about the ferry model, used controllers, path following and parameter estimation methods. In chapter 3 the simulation implementation is described and the simulation results, followed by the results of using parameter estimations in the controllers. In chapter 4 the conclusion and future work is presented.

Chapter 2

Theory

An overview of the theory and methods used in the simulations is presented in this chapter.

2.1 Modeling

The model of the ferry is based on a six Degrees of freedom (DOF) rigid-body which is simplified by neglecting heave, roll and pitch, assuming they are small. This results in a 3 DOF model with the states surge, sway and yaw giving the kinematics

$$\dot{\boldsymbol{\eta}} = \mathbf{R}(\psi)\boldsymbol{\nu} \tag{2.1}$$

with the state vectors $\boldsymbol{\eta} = [x, y, \psi]^T$, $\boldsymbol{\nu} = [u, v, r]^T$. It is important to keep in mind which coordinate system each vector is placed in. The pose vector $\boldsymbol{\nu}$ is represented in the North-East-Down (NED) frame, where the x axis points to true north, y axis to east and z points downwards. The NED coordinate system is a tangential plane from where the origin is placed, and does not take the earths curving into account. Since operation of the autonomous ferry will be in a local area this does not effect navigation.

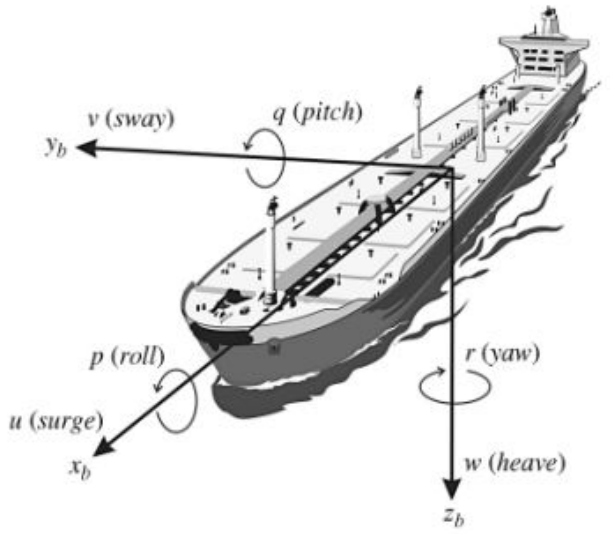

Figure 2.1: Illustration of the coordinate system in body (Fossen, 2011)

The body frame is shown in Figure 2.1, where the moving coordinate system is fixed to the ferrys positioning and heading. The origin is placed on the ferry, with the x axis pointing in the longitudinal direction of the vessel, y axis in the transverse direction and the z axis normal on x and y axis and pointing downwards. The rotation matrix transform coordinates from body to the NED frame, and is simplified to

$$\mathbf{R}(\psi) = \begin{bmatrix} cos(\psi) & -sin(\psi) & 0 \\ sin(\psi) & cos(\psi) & 0 \\ 0 & 0 & 1 \end{bmatrix} \tag{2.2}$$

The kinetics of the ferry is described from (Fossen, 2011) on the form

$$\mathbf{M}\dot{\boldsymbol{\nu}} + \mathbf{C}(\boldsymbol{\nu})\boldsymbol{\nu} + \mathbf{D}(\boldsymbol{\nu})\boldsymbol{\nu} = \boldsymbol{\tau} + \boldsymbol{\tau}_{wind} + \boldsymbol{\tau}_{wave} \tag{2.3}$$

with the matrices

$$\mathbf{M} = \begin{bmatrix} m_{11} & m_{12} & m_{13} \\ m_{21} & m_{22} & m_{23} \\ m_{31} & m_{32} & m_{33} \end{bmatrix} \tag{2.4a}$$

$$\mathbf{C}(\boldsymbol{\nu}) = \begin{bmatrix} 0 & 0 & c_{13}(\boldsymbol{\nu}) \\ 0 & 0 & c_{23}(\boldsymbol{\nu}) \\ c_{31}(\boldsymbol{\nu}) & c_{32}(\boldsymbol{\nu}) & 0 \end{bmatrix} \tag{2.4b}$$

$$\mathbf{D}(\boldsymbol{\nu}) = \begin{bmatrix} d_{11}(\boldsymbol{\nu}) & d_{12} & d_{13} \\ d_{21} & d_{22}(\boldsymbol{\nu}) & d_{23}(\boldsymbol{\nu}) \\ d_{31} & d_{32}(\boldsymbol{\nu}) & d_{33}(\boldsymbol{\nu}) \end{bmatrix} \tag{2.4c}$$

where $\mathbf{C}(\boldsymbol{\nu})$ is dependent on the inertia matrix $\mathbf{M}$

$$c_{13}(\boldsymbol{\nu}) = -m_{12}u - m_{22}v - m_{23}r \tag{2.5a}$$
$$c_{23}(\boldsymbol{\nu}) = m_{11}u \tag{2.5b}$$
$$c_{31}(\boldsymbol{\nu}) = -c_{13}(\boldsymbol{\nu}) \tag{2.5c}$$
$$c_{32}(\boldsymbol{\nu}) = -c_{23}(\boldsymbol{\nu}) \tag{2.5d}$$

and the elements of $\mathbf{D}(\boldsymbol{\nu})$ are defined as

$$d_{11}(\boldsymbol{\nu}) = -X_u - X_{|u|u}|u| - X_{uuu}u^2 \tag{2.6a}$$
$$d_{12} = -X_v \tag{2.6b}$$
$$d_{13} = -X_r \tag{2.6c}$$
$$d_{21} = -Y_u \tag{2.6d}$$
$$d_{22}(\boldsymbol{\nu}) = -Y_v - Y_{|v|v}|v| - Y_{|r|v}|r| - Y_{vvv}v^2 \tag{2.6e}$$
$$d_{23}(\boldsymbol{\nu}) = -Y_r - Y_{|v|r}|v| - Y_{|r|r}|r| \tag{2.6f}$$
$$d_{31} = -N_u \tag{2.6g}$$
$$d_{32}(\boldsymbol{\nu}) = -N_v - N_{|v|v}|v| - N_{|r|v}|r| \tag{2.6h}$$
$$d_{33}(\boldsymbol{\nu}) = -N_r - N_{|v|r}|v| - N_{|r|r}|r| - N_{rrr}r^2 \tag{2.6i}$$

From (2.6), $\mathbf{D}(\boldsymbol{\nu})$ can be divided into a linear and nonlinear part, $\mathbf{D}(\boldsymbol{\nu}) = \mathbf{D}_L + \mathbf{D}_{NL}(\boldsymbol{\nu})$.

The model parameters in $\mathbf{M}$, $\mathbf{C}$ and $\mathbf{D}$ has been estimated by optimizing a least error algorithm to find the most accurate parameters fitting with the test data, (Pedersen, 2019).

2.2 Navigation and Control

It is implemented a simple guidance system with a reference filter to navigate between waypoints. The performance of three controllers is tested. The different controllers that have been tested give different results when taking into account tracking error, thruster usage and dealing with disturbances and model discrepancies. The tested controllers were variations of the PID controller and adaptive methods with reference feedforward.

2.2.1 PID controller with model reference feedforward

The PID controller is formulated in the body frame, with the error in the NED frame rotated. The transposed of the rotational matrix with the error gives $e = R(\psi)(\eta_d - \eta)$ and $\dot{e} = \nu_d - \nu$. From this the PID controller derives to

$$\boldsymbol{\tau}_{PID} = \mathbf{K_p e} + \mathbf{K_i} \int_0^t \mathbf{e} d\mu + \mathbf{K_d \dot{e}}. \tag{2.7}$$

Referenced feedforward uses the desired velocity and acceleration to calculate the "correct" $\boldsymbol{\tau}$ given the vessel model in (2.3). This gives a predicted $\boldsymbol{\tau}$ to keep the desired trajectory, which leaves the PID controller to compensate for modeling errors. The feedforward force is given by

$$\boldsymbol{\tau}_{FF} = \mathbf{M}\dot{\boldsymbol{\nu}}_d + \mathbf{C}(\boldsymbol{\nu}_d)\boldsymbol{\nu}_d + \mathbf{D}(\boldsymbol{\nu}_d)\boldsymbol{\nu}_d. \tag{2.8}$$

The resulting control input of the PIDwFF is then

$$\boldsymbol{\tau}_{PID} = \mathbf{M}\dot{\boldsymbol{\nu}}_d + \mathbf{C}(\boldsymbol{\nu}_d)\boldsymbol{\nu}_d + \mathbf{D}(\boldsymbol{\nu}_d)\boldsymbol{\nu}_d + \mathbf{K_p e} + \mathbf{K_i} \int_0^t \mathbf{e} d\mu + \mathbf{K_d \dot{e}}. \tag{2.9}$$

2.2.2 Adaptive backstepping controller

The ABC is derived from a backstepping method where it is assumed discrepancies in all matrices of the model in (2.3), represented by the pertubations δ, σ and ρ, in addition to an external force ω:

$$\delta\mathbf{M}\dot{\boldsymbol{\nu}} + \delta\mathbf{C}(\boldsymbol{\nu})\boldsymbol{\nu} + \sigma\mathbf{D}(\boldsymbol{\nu})\boldsymbol{\nu} = \rho\boldsymbol{\tau} + \mathbf{R}(\psi)^T\omega. \tag{2.10}$$

This model is used to derive a backstepping controller. When choosing the control law all the model discrepancies were simplified to be represented through the external forces. This simplification gives estimates of forces working on the ferry in any directions, but can not represent changes in the damping or inertia matrices which happens with changes of the load. This controller works in a similar manner as PIDwFF with the adaptive term, $\boldsymbol{\omega}$, acting as integral force with quicker adaptation. The control law from backstepping is run through a low-pass filter to remove the high oscillations that is created by the adaptive method, resulting in

$$\boldsymbol{\tau}_{adp} = -\mathbf{R}(\psi)^T\hat{\boldsymbol{\omega}}_\delta + \mathbf{M}\dot{\boldsymbol{\alpha}} + \mathbf{C}\boldsymbol{\alpha} + \mathbf{D}\boldsymbol{\alpha} - \mathbf{z_1} - \mathbf{K_2 z_2} \tag{2.11}$$

where

$$\dot{\hat{\boldsymbol{\omega}}}_\delta = -\gamma_{\omega_\delta}\mathbf{R}\tilde{\boldsymbol{\nu}}$$

$$\boldsymbol{\alpha} = -\mathbf{K_1 z_1} + \mathbf{R}^T\dot{\boldsymbol{\eta}}_d$$

$$\mathbf{z_1} = \mathbf{R}^T(\boldsymbol{\eta} - \boldsymbol{\eta}_d)$$

$$\mathbf{z_2} = \boldsymbol{\nu} - \boldsymbol{\alpha}.$$

With this adaptive method the update laws for the estimates of the model discrepancies, found in (2.11), are chosen so that they would converge through Lyapunov analysis (Sæther, 2019).

2.2.3 PD controller with adaptive feedforward

When implementing the PDwAFF, (2.8) is used for finding τ. In addition the external forces is found by implementing the adaptive term $\boldsymbol{\omega}$ from the ABC. This makes it able to compensate for disturbances and some of the discrepancies of the model. The same update law for $\hat{\omega_\delta}$ is used as in the ABC. This makes the PDwAFF as follows

$$\boldsymbol{\tau}_{PD_{FF}} = -\mathbf{R}^T\hat{\boldsymbol{\omega}}_\delta + \mathbf{M}\dot{\boldsymbol{\nu}} + \mathbf{C}(\boldsymbol{\nu}_d)\boldsymbol{\nu}_d + \mathbf{D}(\boldsymbol{\nu}_d)\boldsymbol{\nu}_d + \mathbf{K_p e} + \mathbf{K_d}\dot{\mathbf{e}} \tag{2.12}$$

When Adding the adaptive part in the feedforward, This acts as the integral action in the controller. So if there are constant disturbances they are compensated for in $\hat{\boldsymbol{\omega}}_\delta$. Therefore only a PD controller is used with the adaptive feedforward.

2.2.4 Reference filter

A third order reference filter is implemented to ensure smooth an continuous signals for the desired position, velocity and acceleration. If a step on the desired position is given the reference filter gives a feasible signal for the ferry to follow. From the reference($\mathbf{r}$) to the desired position($\boldsymbol{\eta}$) the transformation is given in (Fossen, 2011) on the form

$$\boldsymbol{\eta}_d^{(3)} + (2\Delta + \mathbf{I})\Omega\ddot{\boldsymbol{\eta}}_d + (2\Delta + \mathbf{I})\Omega^2\dot{\boldsymbol{\eta}}_d + \Omega^3\boldsymbol{\eta}_d = \Omega^3\mathbf{r}. \tag{2.13}$$

2.2.5 Line of sight navigation

To navigate through a set of waypoints a Line of sight (LOS) guidance system can be used to give a desired position and heading (Fossen, 2011). This enables path following for the ferry so that it can reach the docking on each side. A LOS with enclosure based steering is used to reach the waypoints. This is done by following a straight line between the previous waypoint to the next. A circle of acceptance is created around the ferry and where it intercepts with the line between the waypoints gives the desired position, shown

in Figure 2.2. The desired heading is found from the angle of the LOS vector. When the next waypoint is within the circle of acceptance it navigates to the next waypoint.

The desired position and heading is given by

$$x_d = x_{los} \tag{2.14a}$$
$$y_d = y_{los} \tag{2.14b}$$
$$\psi_d = \text{atan2}(y_{los} - y(t), x_{los} - x(t)) \tag{2.14c}$$

where y_{los} and x_{los} are found by solving the equation set

$$R^2 = [x_{los} - x(t)]^2 + [y_{los} - y(t)]^2 \tag{2.15}$$
$$tan(\alpha_k) = \frac{y_{k+1} - y_k}{x_{k+1} - x_k} = \frac{y_{los} - y_k}{x_{los} - x_k} \tag{2.16}$$

The solution to these equations are found in (Fossen, 2011)(10.70 and 10.71), with conditions for which solution to the 2nd order equations to use depending on current and next waypoint.

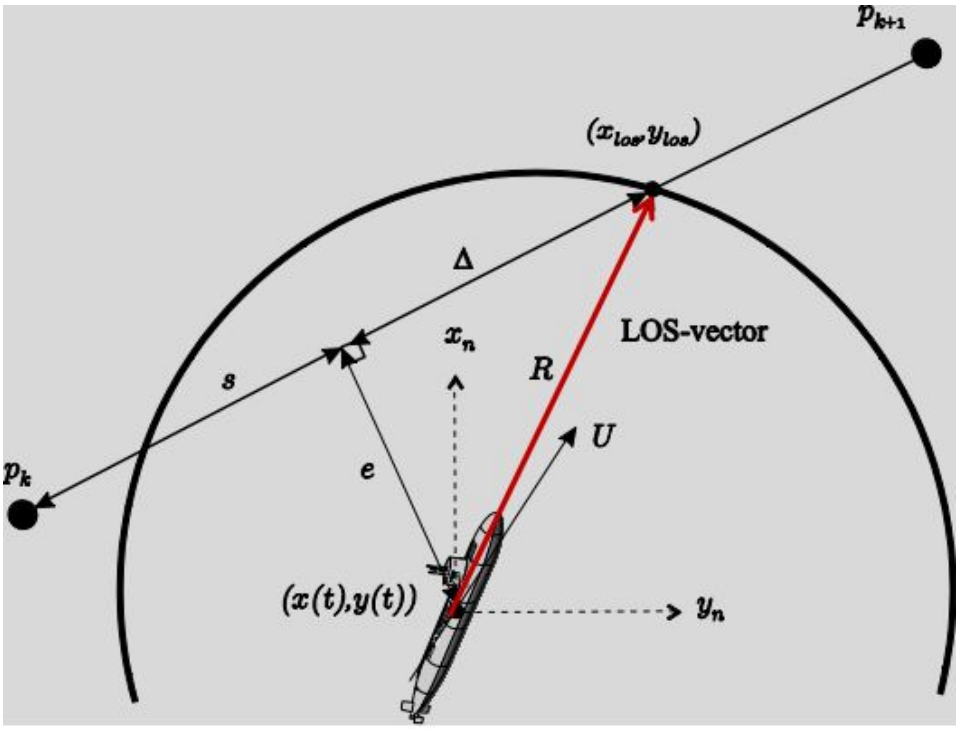

Figure 2.2: LOS vector from intersection between circle of acceptance and waypoint line. Courtesy of (Fossen, 2011).

2.3 Online parameter estimation

To achieve online parameter estimation it is possible to use an output error identification method. By looking at the error between the model and the actual output it is possible to converge the estimated parameters towards the real value, by using excitation in the input, (Ioannou and Sun, 1996). This can be used to get better estimates of the parameters in the model. A persistent excitation in the input signal is required, ensuring that all states are excited, to achieve a full convergence between the estimated and actual parameters. This can become a problem since nominal control would not necessary excite all the states as much.

From a parameterized model of the system, $\boldsymbol{\theta}$ is the parameters to be estimated. An update law for the estimated $\boldsymbol{\theta}(t)$ must be found to make the estimated values converge towards the real ones($\boldsymbol{\theta}^*$). There are different update methods for $\dot{\boldsymbol{\theta}}$ that are designed using stability analysis or optimization techniques. These methods aim to minimize the error between measured and estimated output, and assume that when the output error goes to zero the estimates($\boldsymbol{\theta}$) converge towards the real parameters($\boldsymbol{\theta}$* (Ioannou and Sun, 1996). Two used methods are gradient and least-squares algorithms. The normalized estimation error(ϵ) is given as the error between the measurement(z) and the estimated parameters($\hat{z}$).

$$z = \theta^{*T}\phi \tag{2.17}$$

$$\hat{z} = \theta^{T}\phi \tag{2.18}$$

$$\epsilon = \frac{z - \hat{z}}{m^2} \tag{2.19}$$

In (2.19) $m^2 = 1 + n_s^2$ and n_s^2 is chosen to keep ϵ bounded (e.g., $n_s^2 = \phi^T\phi$).

2.3.1 Gradient methods

This method uses simple optimization techniques to minimize a cost function. The cost function are variations of expressions of the error. Together with Lyapunov analysis, these update laws are proved with global asymptotic stability properties, if the input is PE

Instantaneous cost

The gradient method using instantaneous cost is the simplest update law. With a quadratic cost function

$$\mathbf{J}(\boldsymbol{\theta}) = \frac{\epsilon^2 m^2}{2} = \frac{(z - \boldsymbol{\theta}^T\boldsymbol{\phi})^2}{2m^2}, \tag{2.20}$$

the gradient of the cost function updates the estimates of θ. Hence $\mathbf{J}(\theta)$ goes towards the global minimum. The gradient of the cost function is given by

$$\nabla\mathbf{J}(\boldsymbol{\theta}) = -\frac{(z - \boldsymbol{\theta}^T\boldsymbol{\phi})\boldsymbol{\phi}}{m^2} = -\epsilon\boldsymbol{\phi} \tag{2.21}$$

By implementing an adaptive gain, $\mathbf{\Gamma} = \mathbf{\Gamma}^T > 0$, the adaptive law for updating $\boldsymbol{\theta}(t)$ is found from the gradient method.

$$\dot{\boldsymbol{\theta}} = -\mathbf{\Gamma}\nabla\mathbf{J}(\boldsymbol{\theta}) \tag{2.22}$$

$$\dot{\boldsymbol{\theta}} = \mathbf{\Gamma}\epsilon\boldsymbol{\phi} \tag{2.23}$$

With a convex $\mathbf{J}(\theta)$ this guaranties the existence of a single global minimum. The properties of this method is bounded ϵ and θ, and exponentially convergence for $\theta(t)$ to θ^* if ϕ is PE.

Integral cost

The integral cost function utilizes a forgetting factor, $\beta > 0$, and chooses the parameter θ to minimize the integral square error of the past data. The forgetting factor discards data that is old enough exponentially. the integral cost function is

$$\mathbf{J}(\theta) = \frac{1}{2}\int_0^t e^{-\beta(t-\tau)}\epsilon^2(\tau)m^2(\tau)d\tau \tag{2.24}$$

$\mathbf{J}(\theta)$ is convex also in (2.24), so minimizing using the gradient method w.r.t θ finds the global minimum. This gives the update law

$$\dot{\boldsymbol{\theta}} = -\mathbf{\Gamma}\nabla\mathbf{J} = \mathbf{\Gamma}\int_0^t e^{-\beta(t-\tau)}\frac{(z(\tau) - \boldsymbol{\theta}^T\boldsymbol{\phi}(\tau))}{m^2(\tau)}\boldsymbol{\phi}(\tau)d\tau \tag{2.25}$$

Where $\mathbf{\Gamma} = \mathbf{\Gamma}^T > 0$ is the adaption gain, and β the forgetting factor. The update law (2.25) can be implemented as

$$\dot{\boldsymbol{\theta}} = -\mathbf{\Gamma}(\mathbf{R}(t)\boldsymbol{\theta} + \mathbf{Q}(t)) \tag{2.26a}$$

$$\dot{\mathbf{R}} = -\beta\mathbf{R} + \frac{\boldsymbol{\phi}\boldsymbol{\phi}^T}{m^2}, \qquad \mathbf{R}(0) = 0 \tag{2.26b}$$

$$\dot{\mathbf{Q}} = -\beta\mathbf{Q} - \frac{z\boldsymbol{\phi}}{m^2}, \qquad \mathbf{Q}(0) = 0 \tag{2.26c}$$

This results in the same stability proofs for the minimum of $\mathbf{J}(\boldsymbol{\theta})$ with global asymptotic stability, with $\boldsymbol{theta}$ converging to $\boldsymbol{\theta}^*$.

2.3.2 Least-squares

The least-squares algorithm uses the sum of the squares from the error between the modeled and measured data to update the mathematical model. By using this method the noise or inaccuracies in the measurements are expected to have less effect. This is a versatile method which can be equipped with covariance resetting and forgetting factor to help

faster convergence and adaptation against changes. The update law of θ uses a matrix $\mathbf{P}$ acting as a covariance matrix, and is found by the cost function

$$\mathbf{J}(\boldsymbol{\theta}) = \frac{1}{2}\int_0^t e^{-\beta(t-\tau)}\frac{(z(\tau)-\boldsymbol{\theta}^T\boldsymbol{\phi}(\tau))^2}{m^2(\tau)}d\tau + \frac{1}{2}e^{-\beta(t)}(\boldsymbol{\theta}-\boldsymbol{\theta}_0)^T\mathbf{Q}_0(\boldsymbol{\theta}-\boldsymbol{\theta}_0) \quad (2.27)$$

Hence $\mathbf{J}(\boldsymbol{\theta})$ is convex the global minimum is given by $\mathbf{J}(\boldsymbol{\theta}) = 0$, where the gradient of $\mathbf{J}(\boldsymbol{\theta})$ is

$$\nabla\mathbf{J}(\boldsymbol{\theta}) = e^{-\beta t}\mathbf{Q}_0(\boldsymbol{\theta}(t)-\boldsymbol{\theta}_0) - \int_0^t e^{-\beta(t-\tau)}\frac{(z(\tau)-\boldsymbol{\theta}^T\boldsymbol{\phi}(\tau))}{m^2(\tau)}\boldsymbol{\phi}(\tau)d\tau \quad (2.28)$$

The solution to the global minimum yields

$$\boldsymbol{\theta}(t) = \mathbf{P}(t)[e^{-\beta t}\mathbf{Q}_0\boldsymbol{\theta}_0 + \int_0^t e^{-\beta(t-\tau)}\frac{z(\tau)\boldsymbol{\phi}(\tau)}{m^2(\tau)}d\tau] \quad (2.29)$$

where

$$\mathbf{P}(t) = [e^{-\beta t}\mathbf{Q}_0 + \int_0^t e^{-\beta(t-\tau)}\frac{\boldsymbol{\phi}(\tau)\boldsymbol{\phi}^T(\tau)}{m^2(\tau)}d\tau] \quad (2.30)$$

$\mathbf{P}(t)$ exists as $\mathbf{Q}_0 = \mathbf{Q}_0^T > 0$ and $\boldsymbol{\phi}\boldsymbol{\phi}^T \geq 0$. From this the update law with least-squares is

$$\dot{\boldsymbol{\theta}} = \mathbf{P}\epsilon\boldsymbol{\phi} \quad (2.31a)$$

$$\dot{\mathbf{P}} = \beta\mathbf{P} - \mathbf{P}\frac{\boldsymbol{\phi}\boldsymbol{\phi}^T}{m^2}\mathbf{P}, \qquad \mathbf{P}(0) = \mathbf{P}_0 = \mathbf{Q}_0^{-1} \quad (2.31b)$$

Least-squares with covariance resetting

With $\beta = 0$ this method is referred to as pure least-squares. The problem being $\mathbf{P}$ may become arbitrarily small and the convergence will slow down. To prevent this covariance resetting is added, by setting $\mathbf{P}(t) = \mathbf{P}_0$ if $\lambda_{min}(\mathbf{P}(t))$ is smaller than the threshold. This results in an exponential convergence for $\boldsymbol{\theta}(t) -> \boldsymbol{\theta}^*$ if $\boldsymbol{\phi}$ is PE.

Least-squares with forgetting factor

By utilizing $\beta \neq 0$ this works as a forgetting factor for better convergence when the behaviour of the system changes. With $\beta \neq 0$ the problem of $\mathbf{P}$ getting arbitrarily small

is not present, but instead there is a chance of $\mathbf{P} -> \infty$. To prevent this R_0 is used as a upper limit for $\mathbf{P}$, and the updated adaptation law becomes

$$\dot{\boldsymbol{\theta}} = \mathbf{P}\epsilon\boldsymbol{\phi} \tag{2.32a}$$

$$\dot{\mathbf{P}} = \beta\mathbf{P} - \mathbf{P}\frac{\boldsymbol{\phi}\boldsymbol{\phi}^T}{m^2}\mathbf{P}, \qquad if||\mathbf{P}(t)|| \leq R_0 \tag{2.32b}$$

$$\dot{\mathbf{P}} = 0, \qquad otherwise \tag{2.32c}$$

This ensure exponentially convergence towards $\boldsymbol{\theta}^*$ when $\boldsymbol{\phi}$ is PE.

2.3.3 Discussion

The four estimation methods uses different update laws for $\boldsymbol{\theta}$. Instantaneous cost is the simplest only taking into account the latest measurement. An improved version of this is integral cost where the integral of ϵ is used to update $\boldsymbol{\theta}$. With the system being a Multiple input multiple output (MIMO) system with nonlinear terms it could be beneficial to use more than the latest measurement, as if there is a constant deviation between $\boldsymbol{\theta}$ and $\boldsymbol{\theta}^*$ this could be corrected with integral cost.

With the least-squares method they have the benefit of using a covariance matrix. This makes the methods able to do more rapid changes to $\boldsymbol{\theta}$ if it is larger variations in ϵ. When the error becomes small and stabilizes the covariance matrix should follow, allowing less changes to $\boldsymbol{\theta}$.

Integral cost and Least-squares with forgetting factor (LSwFF) both has a forgetting factor. This makes them more suitable to adapt to changes that arise, like sudden changes in the model. Least-squares (LS) which does not use forgetting factor will then converge slower towards the changes parameters, as all of the previous measurements with around the old parameters is still remembered.

2.4 Parameters to identify

The ship model is a nonlinear MIMO system, which brings much more complexity to identifying parameters than a single input single output (SISO) system. To be able to use the online estimator schemes described above, some simplifications to the model must be done. Since the ferry has an instability in heading, parameter estimations can not be done on matrix form as a whole system. Each state must therefore be divided and threated as an individual estimation. By using the decoupled model of the ferry the estimations will be done easier. The decoupled model is obtained by putting all coupling terms for surge to zero in $\mathbf{M}$ and $\mathbf{D}$ in (2.3). Each equation for each state can then be found.

$$m_{11}\dot{u} + c_{13}r + (d_{11L} + d_{11NL})u = \tau_u \quad (2.33a)$$
$$m_{22}\dot{v} + m_{23}\dot{r} + c_{23}r + (d_{22L} + d_{22NL})v + (d_{23L} + d_{23NL})r = \tau_v \quad (2.33b)$$
$$m_{32}\dot{v} + m_{33}\dot{r} + c_{31}u + c_{32}v + (d_{32L} + d_{33NL})v + (d_{33L} + d_{33NL})r = \tau_r \quad (2.33c)$$

From the system in (2.33) the nonlinear terms and terms effected by other states can be combined to a τ_σ. This gives us a linear inertia and damping term to estimate shown in (2.34). By combining the coupling terms and nonlinear terms to τ, in each state can be viewed as fully decoupled from each other and estimation can be done as for a SISO system. The parameters to be estimated is m_{ii} and d_{ii} giving adaptive linear terms for inertia and damping dynamics to compensate for the changes. The systems for parameter estimation is

$$m_{11}\dot{u} + d_{11L}u = \tau_{u_\sigma} \quad (2.34a)$$
$$m_{22}\dot{v} + d_{22L}v = \tau_{v_\sigma} \quad (2.34b)$$
$$m_{33}\dot{r} + d_{33L}r = \tau_{r_\sigma} \quad (2.34c)$$

where

$$\tau_{u_\sigma} = \tau_u - c_{13}r - d_{11NL}u \quad (2.35a)$$
$$\tau_{v_\sigma} = \tau_v - m_{23}\dot{r} - c_{23}r - d_{22NL}v - (d_{23L} + d_{23NL})r \quad (2.35b)$$
$$\tau_{r_\sigma} = \tau_r - m_{32}\dot{v} - c_{31}u - c_{32}v - (d_{32L} + d_{33NL})v - d_{33NL}r \quad (2.35c)$$

Since the initial parameters are known, these are used in the nonlinear parts to find τ_σ. On the form in (2.34) the estimator schemes described in section 2.3 can be used to find the adaptive parameters.

$$\theta^*_{\mathbf{i}} = \begin{bmatrix} m_{ii} \\ d_{iiL} \end{bmatrix}, \qquad \phi_{\mathbf{i}} = \begin{bmatrix} \dot{x} \\ x \end{bmatrix}, \qquad \mathbf{z_i} = \tau_{x_\sigma} \quad (2.36)$$

for $i \in 1, 2, 3$ and $x \in u, v, r$.

2.5 Integral Absolute Error

IAE is a common way of measuring the performance of a control system. This method shows how close to a reference signal the system is over time. The weighting of the error is equal throughout the whole measurement, meaning the error at a specific time is given by the slope of the graph. So if the value of the IAE is constant over a time period the error is zero. IAE is given by

$$IAE = \int_0^t |e| dt \quad (2.37)$$

Chapter 3

Simulations

3.1 Simulation Implementation

The simulations are done with Matlab with the model implemented in simulink. Here the system with reference filter, the different controllers and the model of the ferry is simulated. The simulations is run at a fixed step size of 0.01 seconds.

3.1.1 Reference signal

The two input signals that are used is a PE input, subsection 3.3.1, and a LOS path follower, subsection 2.2.5. This is given to the reference filter, subsection 2.2.4, so that the reference signal for η, $\dot{\eta}$ and $\ddot{\eta}$ is continuous and smooth. The bandwidth of the filter is chosen low enough for the ferry to be able to follow the desired movement. A realisation of the reference filter in a block diagram is shown in Figure 3.1. To prevent too high velocities and acceleration it is implemented a saturation on the respective states. The saturation is put as a limit in the integral blocks, instead of a saturation on the state, which would give integral wind-up and create large overshoots.

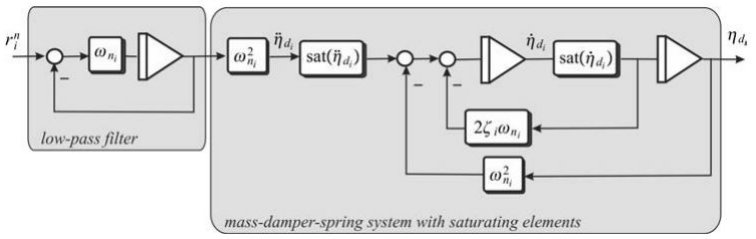

Figure 3.1: Realisation of a 3rd order reference filter in a block diagram, courtesy of (Fossen, 2011)

3.1.2 Line of sight guidance system

The LOS guidance system finds a desired heading by using the function $atan2(y, x)$, which finds the four-quadrant inverse tangent of x and y. This gives a wrapped signal between $\pm 180^\circ$, going from -179° to 179° with only 2° change. The reference filter would then move the heading reference the long way around ta achieve the desired heading. To unwrap the reference signal the error between the new desired heading and the current reference signal is found and added to the current reference signal. This gives a continuous heading reference which is not bounded if the ferry should drive in circles.

3.1.3 Controllers

The three controllers is implemented with a Matlab function which takes input from the signals in simulink. Each controller finds the desired output by calculating the error and system matrices for the feedforward. The output, τ, is fed to the thrusters.

3.1.4 Thrusters

From (Sæther, 2019) it is described a significant delay from a set point is given to the thrusters react to it, as well as having quite slow dynamics when rotating and reaching the desired force. The thruster dynamics have not been modeled so the dynamics is represented by a pure time delay of 0.5 seconds. This is the delay that was estimated for the thrusters to react to a given set point. The thrusters has a saturated output of maximum 500Nm force in any direction and 1000Nm torque when turning. This correspond to the thrusters on milliAmpere.

3.1.5 Model changes

The model of the ferry is derived from testing with stable conditions, with no change of passengers(load) and only small changes in the weather conditions. To simulate how the dynamics of the ship changes from zero to full load the model is altered. Changes in the load is modelled by adding weight in the inertia matrix $\mathbf{M}$. More mass will give an increase of inertia and it is assumed a linear increase of the parameters in $\mathbf{M}$ proportionally to the added weight. Since $\mathbf{C}$ is dependent of the inertia matrix($\mathbf{M}$) the changes of the Coriolis and centripetal matrix are given from the changes of $\mathbf{M}$. The calculation of a new $\mathbf{M}$ is done by specifying a number of passengers with an estimated average weight and calculating a scaling factor(K_M) for $\mathbf{M}$.

$$K_M = \frac{weight_{passengers} + weight_{ferry}}{weight_{ferry}} \tag{3.1}$$

$$M = K_M \cdot M_{initial} \tag{3.2}$$

The same alterations could be done with the damping matrix. Since the damping matrix contains linaer and nonlinear terms some assumptions must be done to how the load affects $\mathbf{D}$. This is not looked into in this thesis.

3.1.6 Parameter estimation

The different parameter estimators is implemented with the methods describes in section 2.3. The estimated parameters are given back to the controllers to update the model. To realise the estimator algorithms a forward Euler method is used to update values, where the change of a parameter is its derivative times the step size.

3.1.7 Estimation difficulties

One of the difficulties when estimating, is the non linear terms of $\mathbf{D}_{NL}$ which can create unwanted affects. The estimators are linear and Only the linear terms of $\mathbf{D}$ can be estimated, so if there is any discrepancies in the nonlinear parameters this must be compensated for in the linear term. To do this it must find a balance between quick estimation to compensate or more robustness with slower convergence.

All of the estimator schemes uses parameters that is estimated in other cost functions. This makes the estimators dependent on the others to find their parameters for it self to estimate the real value exactly. This can cause trouble if other local minimums is found between the estimators, and full stability is hard to reach before a all parameters is almost perfect.

3.2 Simulation results

System identification of the linear parameters in the matrices $\mathbf{M}$ and $\mathbf{D}$ of the model is tested with the methods described in section 2.3. These are tested against each other comparing their convergence rate towards the real values, large oscillations in the estimates while converging and overall robustness against inaccuracies.

Testing of the various system identification methods is done by simulating the decoupled model of the ship and analysing how each method converges to the real values in the model. The tests are done with PE in all the states by combining two sine signals with different amplitude and frequency, which is used as the reference signal for desired position of each state in the 3 DOF. The tuning of the identification methods are done with ideal conditions, assuming the forces acting on ferry are given from the feedback loop of the thrusters. Then the delays in the system and the thruster dynamics does not effect the parameter identification.

The initial guess of the parameters to be estimated are chosen with an error from their real values in the model, and is seen in Table 3.1. The error size is not the same between all of the parameters to make sure the conditions are not identical between the inertial or damping parameters. The inertial matrix parameters has an effect in the identification process of the other states with coupling terms through the Coriolis matrix, especially

when all states are excited at the same time. This could make it difficult estimating the parameters of all states at the same time.

Table 3.1: Initial values and real values when estimating

	Initial value		**Real value**	
Parameter	m_{ii}	d_{ii}	m_{ii}	d_{ii}
$\boldsymbol{\theta}_{11}$	2200	20	2389.7	27.6
$\boldsymbol{\theta}_{22}$	2300	60	2533.9	52.9
$\boldsymbol{\theta}_{33}$	4900	100	5068.9	122.8
$\boldsymbol{\theta}_{23}$	50	-40	62.4	-24.7
$\boldsymbol{\theta}_{32}$	10	-10	28.1	-3.5

3.3 Simulations with PE

3.3.1 Persistent excitation of input

To test how the different methods work an input signal with PE of all states is chosen. The persistence of excitation of the input is a condition to achieve the convergence rate that each method should give, (Bitmead, 1984). To have an input consisting of a rich enough signal, it is possible to combine multiple sine waves with different amplitude and frequency. The reference signal for all of the states consists of a square- combined with two sine signals. A square signal can mathematically be expressed from Fourier series expansion as the infinite sum of sine waves containing the odd-integer harmonic frequencies, (Weisstein, 2018). The resulting reference signal should therefore be able to maintain persistent excitation of the system. The reference model gives the desired position from the reference signal to ensure that the ferry is able to track the desired position.

The square signals are given by

$$g_x(t) = 10 \cdot sgn(sin(0.01t)) \tag{3.3a}$$
$$g_y(t) = 10 \cdot sgn(sin(0.014t)) \tag{3.3b}$$
$$g_\psi(t) = 0.7 \cdot sgn(sin(0.008t)) \tag{3.3c}$$

The input for each state is then

$$x_r(t) = g_x(t) + sin(0.1t) + 3sin(0.03t) \tag{3.4a}$$
$$y_r(t) = g_y(t) + sin(0.1t) + 2sin(0.03t) \tag{3.4b}$$
$$\psi_r(t) = g_\psi(t) + 0.17sin(0.08t) + 0.087sin(0.04t) \tag{3.4c}$$

It was experienced during simulations that if the square signals of $y_r(t)$ and $\psi_r(t)$ triggered at the same time or close to each other the coupled terms had easier to influence the estimation of the other state, slowing down the convergence rate. The desired position and velocity from these signals is

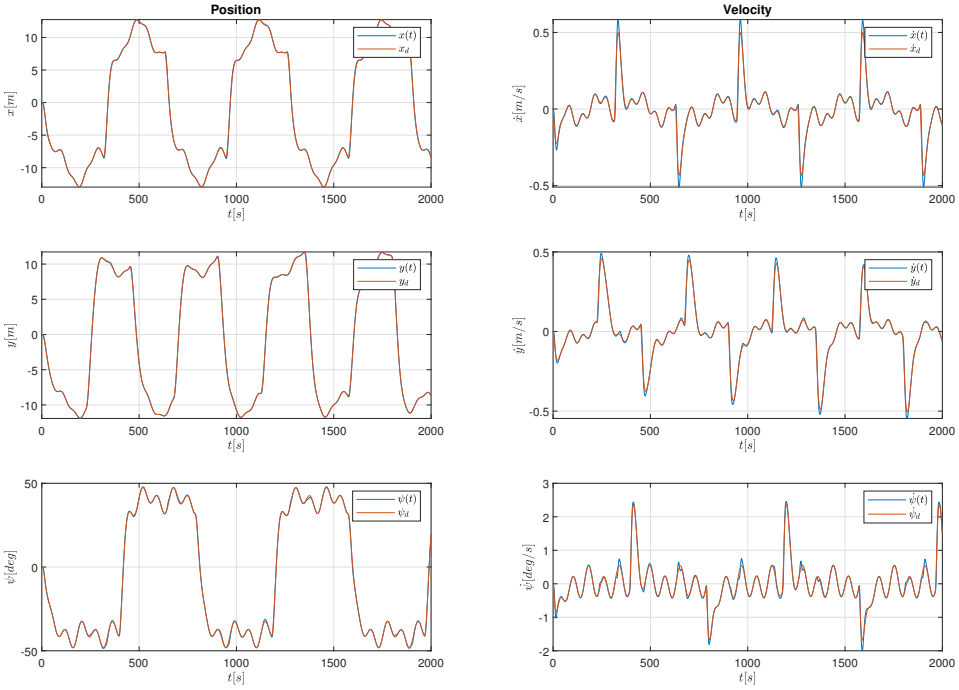

Figure 3.2: Desired position and velocity with PE of system

This gives a moving pattern shown in Figure 3.3, and will achieve PE of the system. The ferry should not use this when in normal operation, but is a way of getting the fastest convergence of the parameters. It could be used as a way to get good initial values with different numbers of passengers, and will be compared with the convergence while simulating nominal driving.

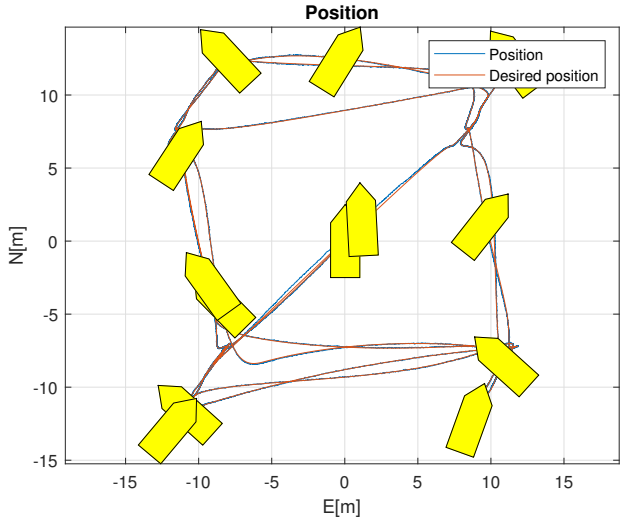

Figure 3.3: Tracking of ferry in north/east with PE of system

3.3.2 Constant coupling terms

The easiest estimations are done when using constant coupling terms in $\mathbf{M}$ and $\mathbf{D}_L$. Only the diagonal of each matrix is estimated giving an adaptive parameter for inertia and damping for each state in $\boldsymbol{\nu}$. With changes to the system matrices the coupling terms will not be estimated, so the parameters on the diagonal will compensate for the other changes to some degree. The initial parameters found in $\mathbf{M}$ also indicate that the diagonal parameters are the most dominant, as in the diagonal parameters of $\mathbf{M}_{initial}$ in (3.5) are much larger than the coupling terms.

$$\mathbf{M}_{initial} = \begin{bmatrix} 2389.7 & 0 & 0 \\ 0 & 2533.9 & 62.4 \\ 0 & 28.1 & 5068.9 \end{bmatrix} \tag{3.5}$$

A simulation with all of the different methods is shown in Figure 3.4.

Instantaneous cost

The simplest of the gradient methods only uses a constant gain to estimate the parameters. Tuning the estimation of the parameters can be done almost individually as they appear decoupled. The model for r has coupling terms depending on the inertia parameters of u and v, effected by $\mathbf{C}$. Hence m_{11} and m_{22} must be close to their real value before the yaw model can converge completely.

With instantaneous cost the parameters modeling u and v converge slower than the other methods. In particular m_{33} and d_{33} are much slower, and it has trouble keeping an exponentially convergence, as the estimates of m_{33} almost stops. The estimate of d_{33}

stays the same for a long time until the square signal for the heading reference triggers. The estimator gains is given by the diagonal matrix $\mathbf{\Gamma}$ and is shown in Table 3.2.

Table 3.2: Estimator parameters for instantaneous cost

Parameter	Value
$\mathbf{\Gamma}_{11}$	diag(150, 1.5)
$\mathbf{\Gamma}_{22}$	diag(150, 3)
$\mathbf{\Gamma}_{33}$	diag(4000, 75)

Integral cost

When implementing integral cost it is a bit more complex with tuning a forgetting factor as well as the gain. The forgetting factor decides the rate of discarding past data. A large β keeps past data for a longer time, and the parameters that are fitted to the model converges slower. In contrast a low β gives more aggressive estimation, only taking into account the last measurements. Therefore β can be used as a damping factor for the estimates.

The convergence rate is some improvement when compared to instantaneous cost. The model parameters for the states u and v reaches the real value faster than the instantaneous cost, but the r parameters give a bad estimate before converging. The positive is that it converges completely with m_{33} before instantaneous cost. the estimator gain Γ and forgetting factor β is shown in Table 3.3

Table 3.3: Estimator parameters for integral cost

Parameter	Value
$\mathbf{\Gamma}_{11}$	diag(3000, 5)
$\mathbf{\Gamma}_{22}$	diag(3000, 5)
$\mathbf{\Gamma}_{33}$	diag(5000, 50)
β_{11}	0.8
β_{22}	0.8
β_{33}	0.2

Least-squares with covariance resetting

The LS method is almost like integral cost but with an adaptive gain($\mathbf{P}$). The adaptive gain has an update law depending on the states and it is difficult to have any control of how $\mathbf{P}$ changes. Without forgetting factor($\beta = 0$) $\mathbf{P}$ is kept from becoming arbitrarily small by resetting $\mathbf{P}$. When simulating there is little control over the covariance matrix($\mathbf{P}$) except for the bounds that are set.

The simulations of the least-squares with covariance resetting show quick convergence with almost always moving closer to the real value. With no forgetting factor, the square er-

ror of all measurements is used. This makes this method less robust to parameter changes, with very good estimates of a static value. This methods gives the quickest convergence with PE and constant coupling terms. The initial covariance matrix and minimum $||\mathbf{P}||$ of this method is shown in Table 3.4.

Table 3.4: Estimator parameters for LS

Parameter	Value
$\boldsymbol{P}_{11}$	diag(1000, 10)
$\boldsymbol{P}_{22}$	diag(3000, 20)
$\boldsymbol{P}_{33}$	diag(10000, 100)
λ_{min11}	1
λ_{min22}	1
λ_{min33}	100

Least-squares with forgetting factor

With forgetting factor the complexity of the tuning increases, with tuning β as a damping factor, and choosing a maximum for the covariance matrix. The complexity makes it difficult to tune so that the convergence is satisfactory. This results in increased convergence time and overshoot compared to the LS method. With the forgetting factor it will be more adaptive to changes, and is similar to integral cost. The initial covariance matrix, maximum $||\mathbf{P}||$ and the forgetting factor is shown in Table 3.5.

Table 3.5: Estimator parameters for LSwFF

Parameter	Value
$\boldsymbol{P}_{11}$	diag(20, 0.1)
$\boldsymbol{P}_{22}$	diag(20, 0.1)
$\boldsymbol{P}_{33}$	diag(500, 10)
β_{11}	1
β_{22}	1
β_{33}	1
R_{max11}	1000
R_{max22}	1000
R_{max33}	10000

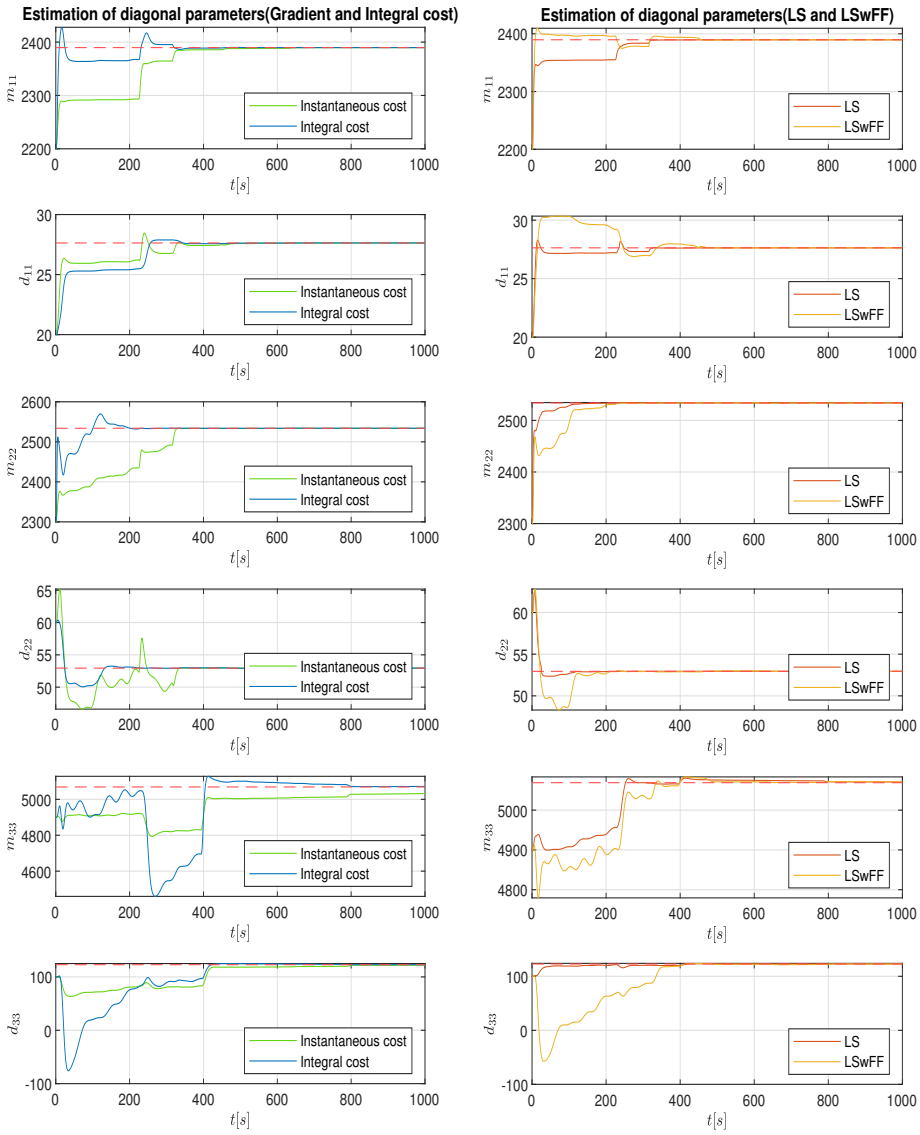

Figure 3.4: Parameter estimation with Persistent excitation and constant coupling terms

3.3.3 Estimated coupling terms

It is possible to estimate the coupled terms with the same methods as above. In the surge decoupled model there are dependencies between v and r, and this parameter can be found by estimating the effect from the coupled state. The challenge when estimating the effect both states have at the same time, is that both parameters will compensate for the same estimation error. Hence the error is corrected for twice, and full convergence to the real parameters is not possible.

To achieve full convergence an iterative solution is used, where the model parameters depending on v and r is not estimated at the same time. This gives independent measurements for each calculation, while using the latest parameter estimations for the coupling terms. The resulting online estimator is more complex with multiple estimated parameters used in all of the estimator schemes. This gives uncertainties in the terms, where one parameter is depending that the other parameters converge to reach the real value. The overall convergence will be slower, but with more exact estimates of more parameters.

With this method the diagonal parameters and the coupling parameters is estimated every other iteration. This gives good convergence rate, with all parameters reaching the real value. The problem with this is if the initial guess of the diagonal parameters are far away from the real value. Then the coupled terms will compensate for the deviations in the other parameters. As the diagonal terms are much larger and more influential in the model, it is beneficial to get good estimates of these before the coupled terms. To implement a faster convergence rate for the diagonal terms, a weighting system is used to give more measurements to estimating these terms. This is done by giving multiple iterations to update the diagonal terms before an iteration is used to update the coupled terms. This gives a quicker convergence of the diagonal parameters, and more stable convergence for the coupled parameters. The coupled parameters then gives a smaller overshoot and error without over compensating to much for the other parameters. The weighting used is five iterations estimating the diagonal of $\mathbf{M}$ and $\mathbf{D}_L$ and one iteration for the coupling terms.

The instantaneous cost method is difficult tuning to satisfaction and with the overall lack of performance compared to the other methods, it was not tested further. The other methods have been tested and compared in Figure 3.5. They give different performances when adding estimation of the coupled terms, and the added complexity makes some of the online estimators hard to tune. In general the overall estimator gains needed to be lower with estimation of the coupling terms.

Integral cost

The integral method is still relatively easy to implement, with a gain and forgetting factor for each parameter pair in $\mathbf{M}$ and $\mathbf{D}_L$. All off the parameters converge approximately exponential with some oscillations until all parameters converge. One of the difficulties with this method is that the coupling terms, and especially m_{23}, moves further away from the initial guess before converging. estimator parameters are shown in Table 3.6.

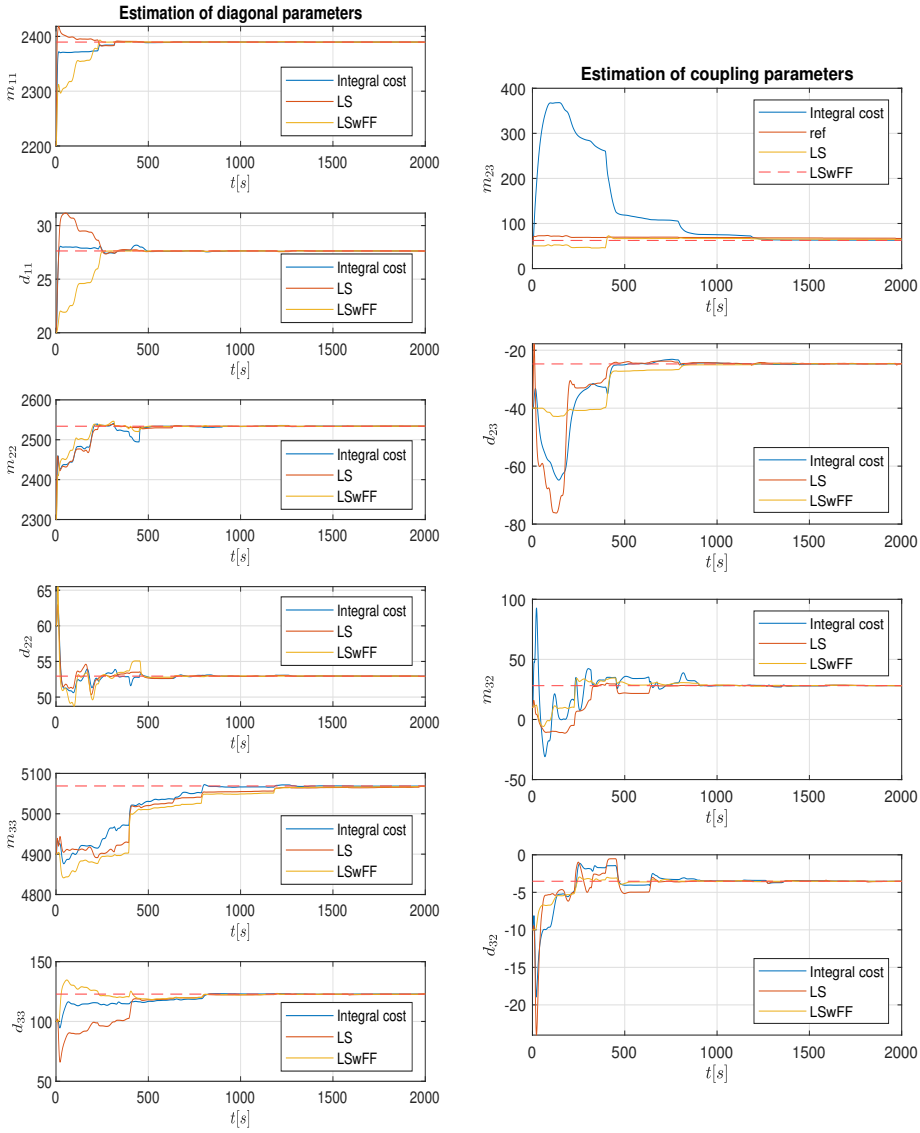

Figure 3.5: Parameter estimation with Persistent excitation and estimated coupling terms

Table 3.6: Estimator parameters for integral cost with estimated coupling terms

Parameter	Value
$\mathbf{\Gamma}_{11}$	diag(400, 4)
$\mathbf{\Gamma}_{22}$	diag(1500, 10)
$\mathbf{\Gamma}_{33}$	diag(10000,100)
$\mathbf{\Gamma}_{23}$	diag(5000, 150)
$\mathbf{\Gamma}_{32}$	diag(5000, 150)
β_{11}	1.2
β_{22}	1.2
β_{33}	1
β_{23}	0.1
β_{32}	0.1

Least-squares with covariance resetting

With the least-squares methods it is harder to control how the estimations are updated. The covariance matrix($\mathbf{P}$) has an update law depending on the states, and only upper or lower bounds of $\mathbf{P}$ can be set. LS which does not have forgetting factor has a slow convergence in most of the parameters. The covariance resetting helps the convergence rate, but still the there is a small deviation which takes long time. It uses long time before the estimates improve, nearly 400 seconds, and has a slower convergence rate than the other methods. The difficult state m_{23} shows the slow convergence rate of the LS method, as there is still a significant deviation between the estimated and true value. In Figure 3.6 the performance of the different methods of estimation m_{23} is shown better. Parameteres used in the estimation is shown in Table 3.7.

Table 3.7: Estimator parameters for LS with estimated coupling terms

Parameter	Value
$\boldsymbol{P}_{11}$	diag(100, 1)
$\boldsymbol{P}_{22}$	diag(300, 2)
$\boldsymbol{P}_{33}$	diag(1000, 20)
$\boldsymbol{P}_{23}$	diag(800, 20)
$\boldsymbol{P}_{32}$	diag(300, 100)
λ_{min11}	0.1
λ_{min22}	1
λ_{min33}	10
λ_{min33}	40
λ_{min33}	1

Least-squares with forgetting factor

LSwFF Shows similar performance as integral cost with quick and stable convergence. With the coupled parameters there is a big improvement and has the smallest deviation to the real values before converging. The problem with the LS also effects the LSwFF method, and is visible in Figure 3.6 as the final convergence is slow. Parameters used in the estimations are shown in Table 3.8.

Table 3.8: Estimator parameters for LSwFF with estimated coupling terms

Parameter	Value
$\boldsymbol{P}_{11}$	diag(100, 0.1)
$\boldsymbol{P}_{22}$	diag(10000, 1)
$\boldsymbol{P}_{33}$	diag(10000, 1)
$\boldsymbol{P}_{23}$	diag(20, 0.5)
$\boldsymbol{P}_{32}$	diag(20, 0.1)
β_{11}	0.1
β_{22}	0.5
β_{33}	0.5
β_{23}	0.4
β_{32}	0.5
R_{max11}	2000
R_{max22}	20000
R_{max33}	20000
R_{max23}	1000
R_{max32}	1000

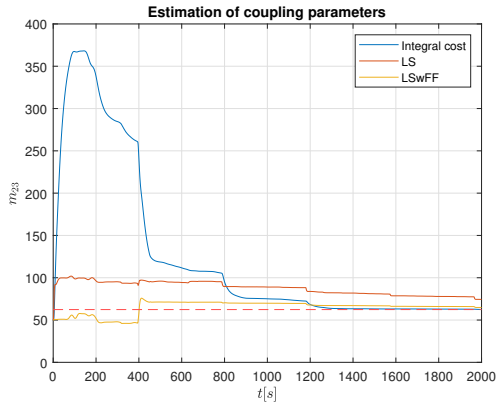

Figure 3.6: Estimation of coupling term m_{23} with PE input

3.4 Simulations with guidance system

3.4.1 Guidance system

One of the challenges with system identification is to excite all the states. While the ferry is driving back and forth this may not happen. To give more realistic simulations it is implemented a LOS enclosure based guidance system to navigate the ferry between two waypoints. This makes it able to see how the parameter estimation will behave under nominal driving.

The LOS guidance system uses two way points that it navigates between, representing each side of the ferry transportation route. The guidance system finds a reference signal for $\mathbf{r}^n = [x_d, y_d, \psi_d]$, that navigates the ferry back and forth. The reference signal is found from the two waypoints and is described in subsection 2.2.5. This gives a path to follow that requires less actuator usage than the PE input, and will result in lower excitation of the system. It should therefore be harder for the estimators to find the true values.

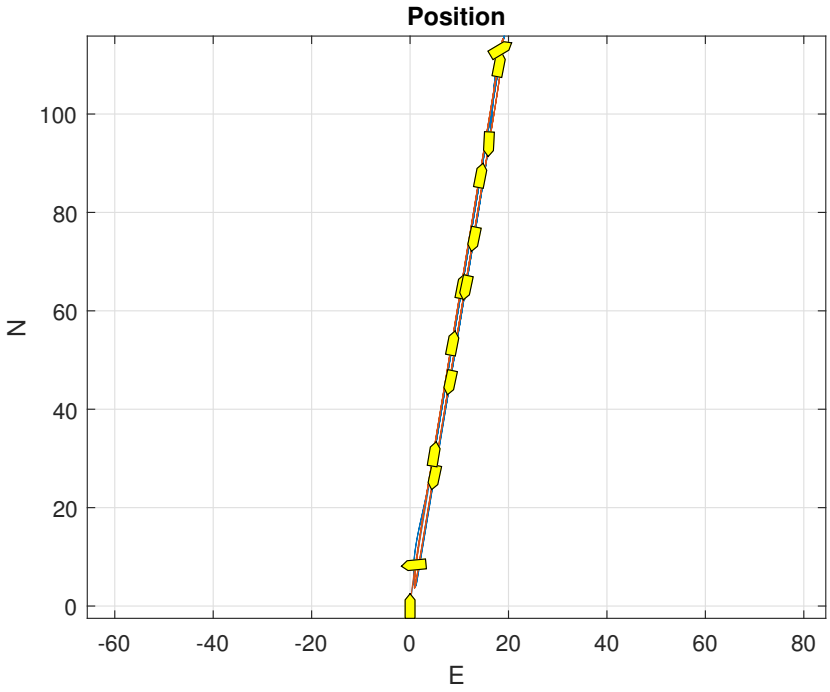

Figure 3.7: LOS guidance system navigating between two waypoints

The guidance system starts in position $(0, 0)$ and goes to $(120, 20)$, giving the movement of the ferry shown in Figure 3.7. With these two waypoints the thrusters give a constant force large parts of the way, and the thrusters does not excite the system very much in these parts.

3.4.2 Constant coupling terms

With constant coupling terms the estimation of the diagonal parameters still converge with all three methods, shown in Figure 3.8. The main difference from the PE input is the period where it moves with constant speed forwards and not exciting the system. This gives no update in the estimated parameters. Only when it reaches a waypoint and turns back around is the system excited and the estimates is updated. In these short periods of turning it is enough to give good estimates within reaching three waypoints.

Integral cost, LS and LSwFF are tested, with all estimates converging. There are some differences, where the LS method has the quickest convergence time comparing with all parameters. With the covariance matrix in the least-squares methods, they suppress the error peaks for the states that have converged already and is influenced by the deviations in the inertia parameters. These are very apparent with the integral cost showing in almost all parameter estimation.

3.4.3 Estimated coupling terms

With estimated coupling terms the estimation takes much longer to reach their real values. Simulations of the different methods is shown in Figure 3.9. The integral cost is with the coupled terms very aggressive, overshooting and creating large spikes while converging. This is similar as without the estimated coupled terms. Despite having large deviations it is one of the fastest to converge completely when all of the parameter estimations come close to their real values, while the least-squares methods have slower and more steady convergence. This is evident in the model parameters of r, m_{32}/d_{32} and m_{33}/d_{33}, when the estimations from integral cost has converged at 3000 seconds and the other methods still has a small error at 5000 seconds.

LS with covariance resetting has the most stable estimates with little to none overshoot and a smooth trajectory when closing in. When considering the model parameters of r this method has more difficulties finding the real parameter value. LSwFF behaves like an improved integral cost, with the forgetting factor giving similar behavior.

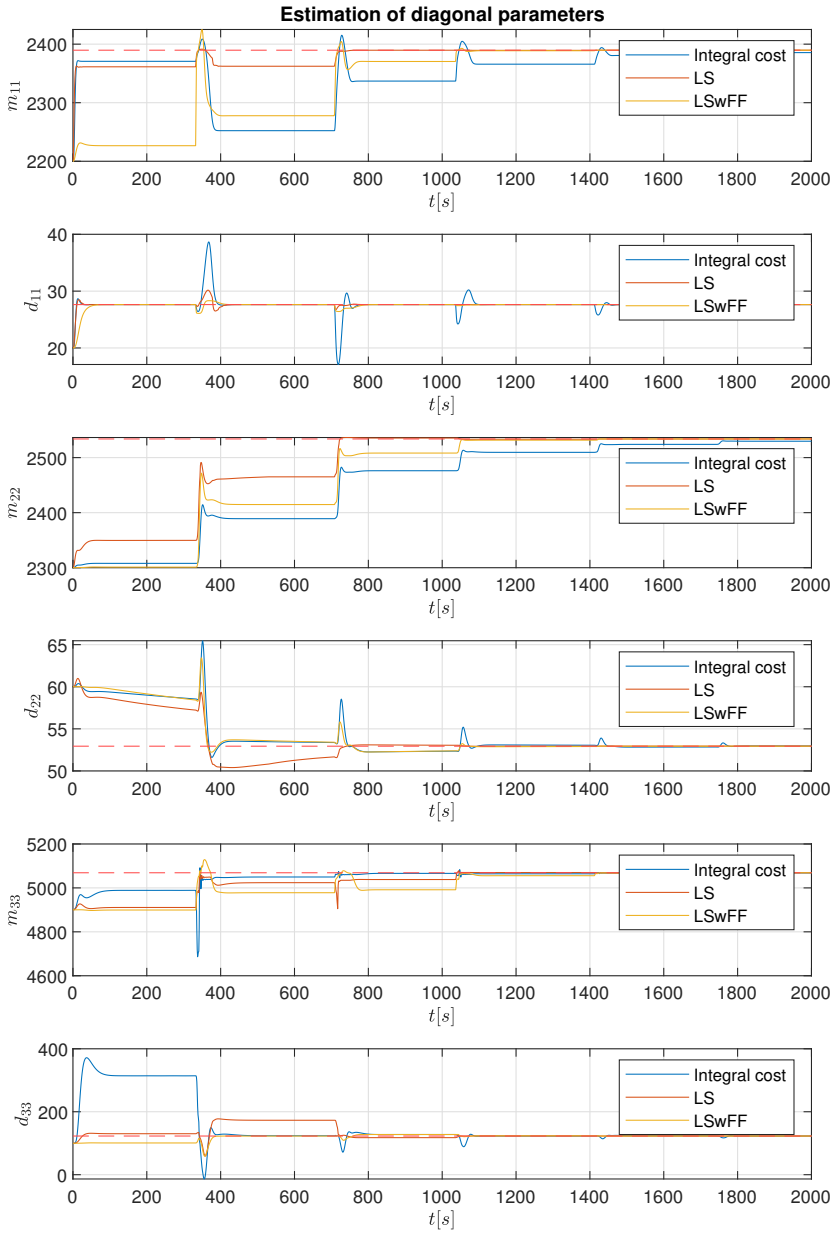

Figure 3.8: Parameter estimation at nominal operation and constant coupling terms

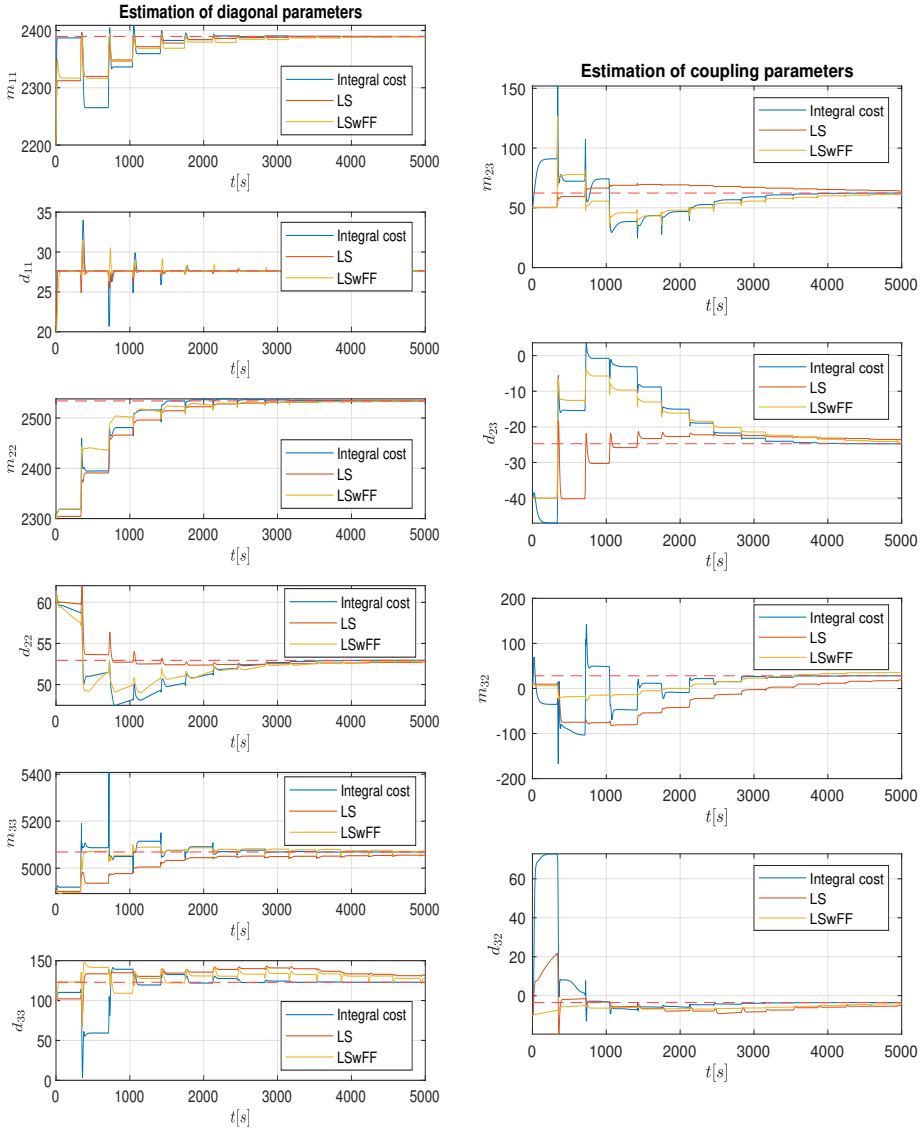

Figure 3.9: Parameter estimation at nominal operation and estimated coupling terms

3.4.4 Continuous estimations

The estimations become more and more time consuming as the complexity with coupled parameters are added and little excitation of the system from nominal driving. each trip with the ferry varies with number of passengers and the ferry can not drive back and forth for 5000 seconds to find the correct parameters every time. Therefore it is necessary to be able to save the estimations and continue the next trip. It is possible to save the estimations for a specific number of passengers or with a pressure sensor measuring the load. If this is implemented on the autonomous ferry it is possible to continue the estimations when the passenger number or load is approximately the same on a trip in the future. With the estimations in Figure 3.9 as an example, the final estimated values could be used as the initial guess for the next period, and continue the convergence. This gives a huge improvement, and the difficult parameters in yaw, m_{33} and d_{33}, are estimated further in Figure 3.10. This shows the possibilities for reaching good estimates after enough trips.

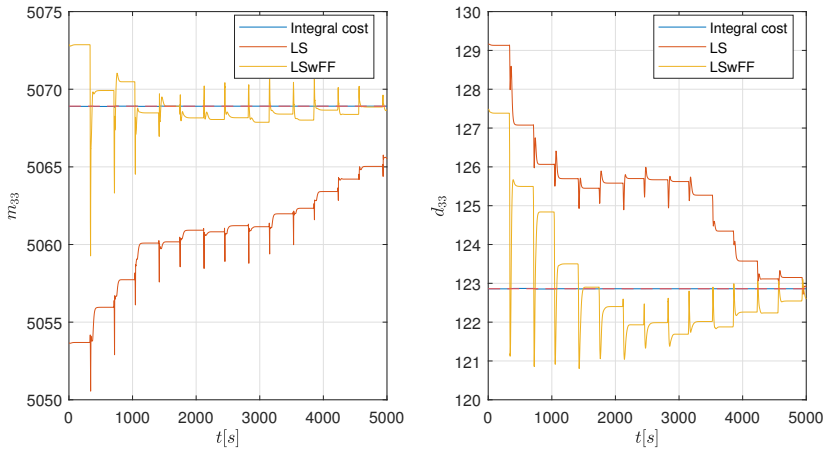

Figure 3.10: Continuous estimation with previous estimated values as initial guess

3.5 Indirect adaptive control

To test if there is any improvement in controlling the ferry, the parameter estimations is used in the controllers with model prediction. This is the PIDwFF, PDwAFF and ABC. The benchmark will be these controllers without any parameter updates, ”no estimation”.They are compared with the controllers using estimated parameter from the different estimation methods. To give a picture of how well the controllers can perform when the parameter estimations have converged, a plot of the controllers with the exact model changes is added, ”perfect estimation”. To compare the results the error and IAE is plotted to see how the error evolves over time. The error is defined as the distance to the desired position and degrees between the heading of the ferry and the desired heading.

The controllers gives a predictive output depending on what reference point is given and the model implemented in the controllers. The implemented model of the controllers is where the parameter updates are done. The test is done with 10 passengers on board. The simulations are run for 10000 seconds, to let the estimations converge and see the effect that this has.

3.5.1 PID with feedforward

With a PIDwFF, the controller without updated parameters gives a small error, with spikes of $0.08m$ and less than 0.5° in error. The implementation of the online system identification with constant coupling terms gives the errors shown in Figure 3.11. This shows the distance error changes little even after the estimated parameters has converged. The biggest improvement is in the heading error. The spikes are reduced exponentially until parameter convergence at approximately 5000 seconds. This is emphasised in Figure 3.12 where the simulation with the exact parameters as in the ferry model, representing a perfect estimation, does not improve the error and performs slightly worse than the simulation without estimation. The improvement of the heading error is much better, where the different methods perform different. Comparing with a perfect estimation all the methods converge to having the same slope, with the LS method giving the quickest convergence. While in the process of finding the estimates the other estimation methods reach parameters that gives a worse error than not estimating any parameters. Once they close in on the estimations, they out perform the original controller.

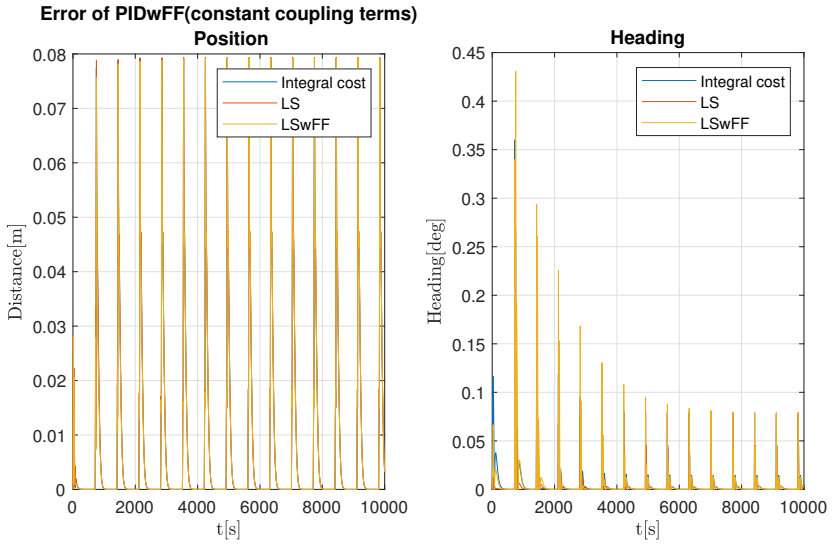

Figure 3.11: Error of position and heading with PID with feedforward and constant coupling terms

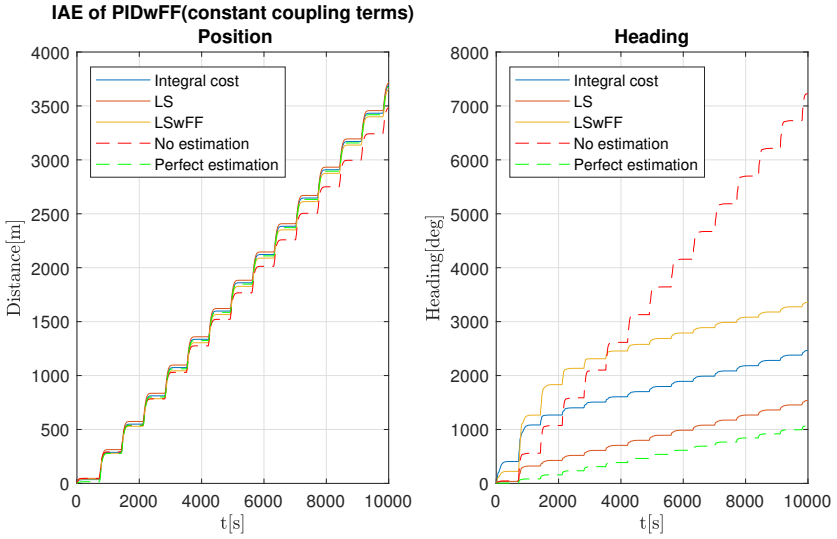

Figure 3.12: IAE of position and heading with PID with feedforward and constant coupling terms

With the methods estimating the coupling terms the IAE is shown in Figure 3.13. The perfect estimation does not improve the distance error compared with when only the diagonal is estimated. Even with a perfect model in the controller there are still errors present. This is caused by the instability of the heading, which is hard to neglect. The complexity of the system gives the integral cost method large deviations which results in a much worse IAE. The LS method performs equally as without the estimated coupling terms. the LSwFF improves the convergence with estimated coupling terms, resulting in an IAE of below $2000°$.

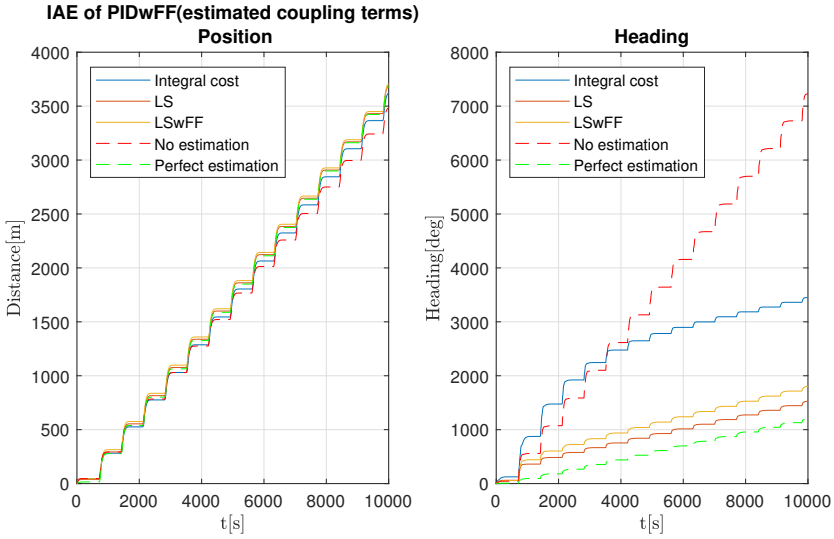

Figure 3.13: IAE of position and heading with PIDwFF and estimated coupling terms

3.5.2 PD with adaptive feedforward

With the adaptive feedforward an adaptive term is used to help compensate for the changes in the dynamics. The error of the distance in Figure 3.14, has similar amplitude of the spikes as the feedforward without adaptive terms. When comparing the heading error spikes it is some improvement, with them converging down to $0.05°$. The main difference is the oscillating between the turning, where the adaptive term is working to neglect the model changes. As the estimations converge the error from the oscillating becomes smaller, but since it is discrepancies between the models from not estimating the coupling terms it does not converge to zero. With estimation of the coupling terms the adaptive term must compensate much less for the model discrepancies. The error is shown in Figure 3.15 where the oscillating error almost disappears completely.

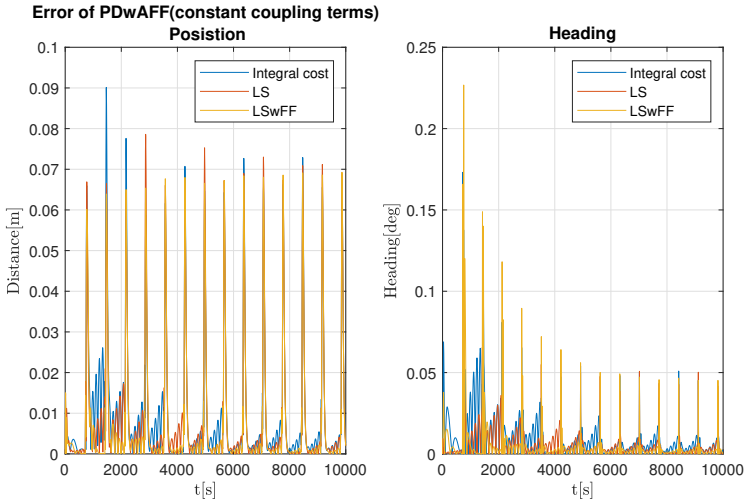

Figure 3.14: Error of position and heading with PD with adaptive feedforward and constant coupling terms

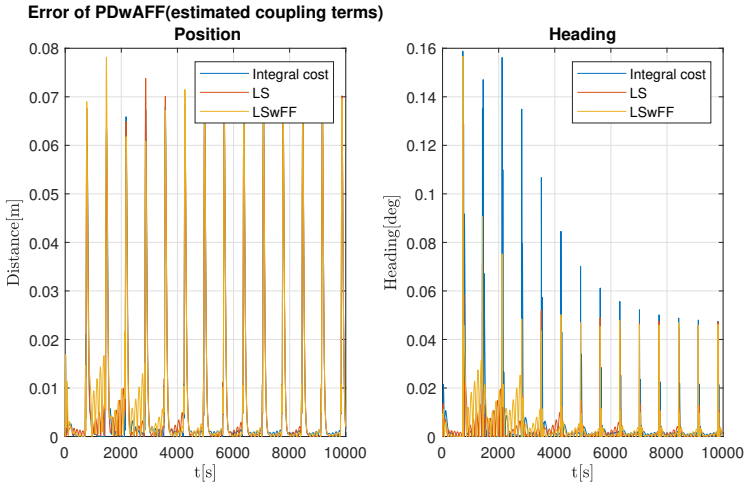

Figure 3.15: Error of position and heading with PDwAFF and estimated coupling terms

This can be seen in the IAE plots of the constant, Figure 3.16, and estimated coupling terms, Figure 3.17. The oscillation from the adaptive term creates a larger IAE without estimating the coupling terms, while with estimation the performance is similar to the the PIDwFF. The heading error has the same effect from the adaptive term. With estimation of the coupling terms the heading error is even less than without the adaptive term. All of the methods converge around 4000 seconds. If the parameters converge to the real values the IAE at 10000 seconds will be bellow $1000°$, further improving the standard PIDwFF.

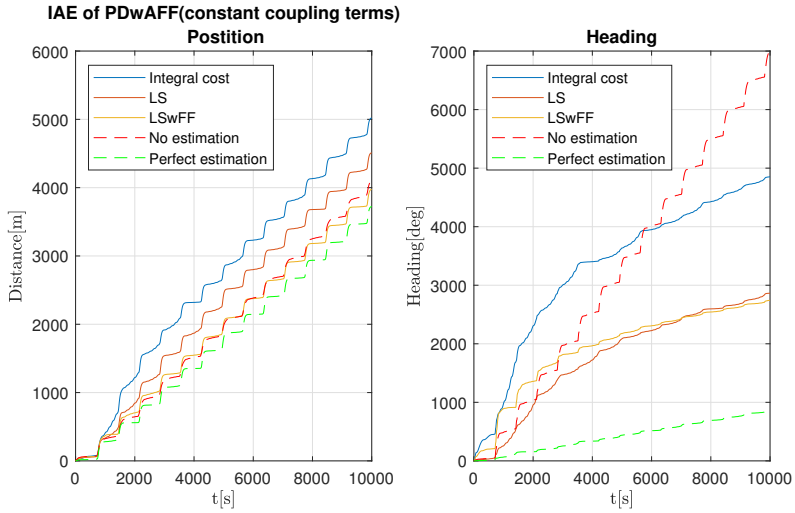

Figure 3.16: IAE of position and heading with PDwAFF and constant coupling terms

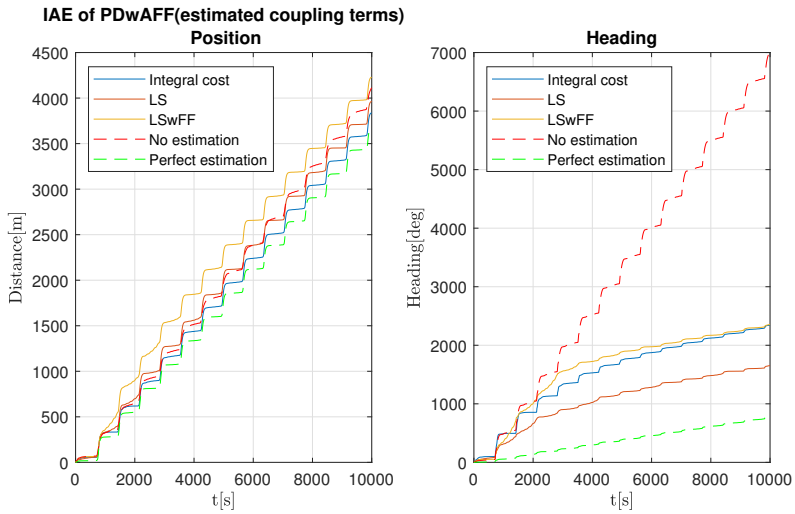

Figure 3.17: IAE of position and heading with PDwAFF and estimated coupling terms

3.5.3 Adaptive backstepping controller

The ABC performs different than the other controllers, where it gives a smaller distance error than heading error. From the error plots in Figure 3.18 and Figure 3.19 it is shown that in both cases converges quickly. The error spikes are improved from the other controllers regarding the distance error with than 0.01 meters, but at the cost of higher heading error spikes of approximately $0.1°$.

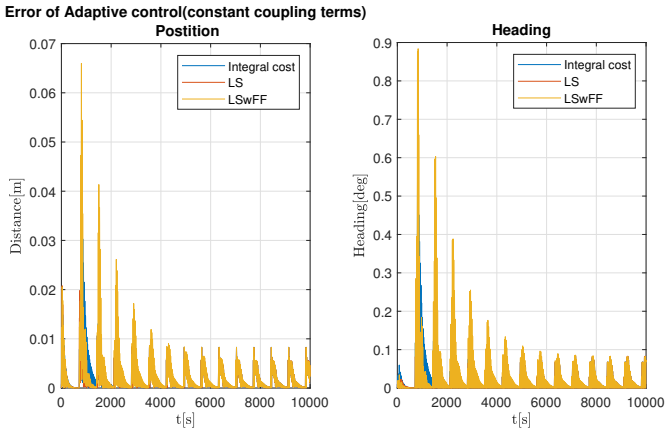

Figure 3.18: Error of position and heading with ABC and constant coupling terms

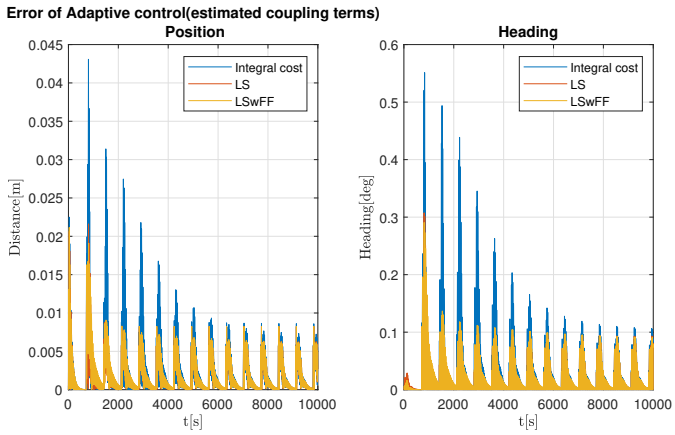

Figure 3.19: Error of position and heading with ABC and estimated coupling terms

When comparing the IAE between the constant and estimated coupling terms in Figure 3.20 and Figure 3.21, it is very little differences. The LS method outperforms the two other methods in both cases, where the LSwFF has worst convergence with constant coupling terms and integral cost struggles with convergence with the added complexity of the estimated coupling terms. The difference between the perfect and no estimation is evident in both cases, giving an improvement of the error. The advantages of estimating the coupling terms is very few when comparing the perfect estimation of both cases. The discrepancies from not estimating the coupling terms does not influence the error allot as the perfect estimation graphs has approximately the same slope. The extra complexity only results in slower convergence while using the ABC.

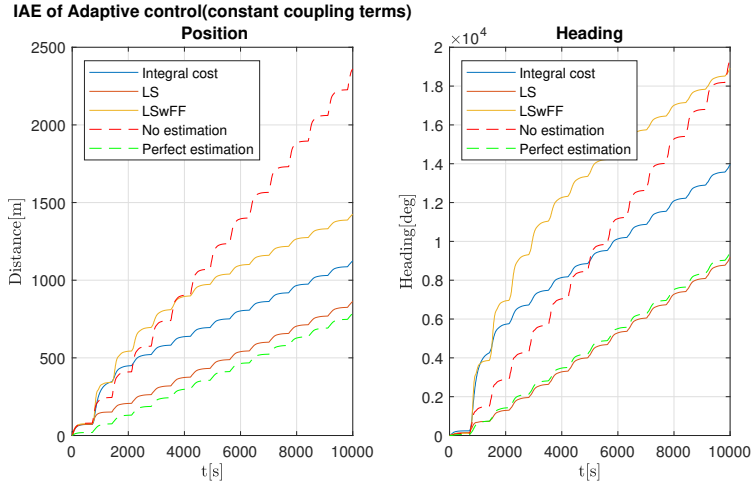

Figure 3.20: IAE of position and heading with ABC and constant coupling terms

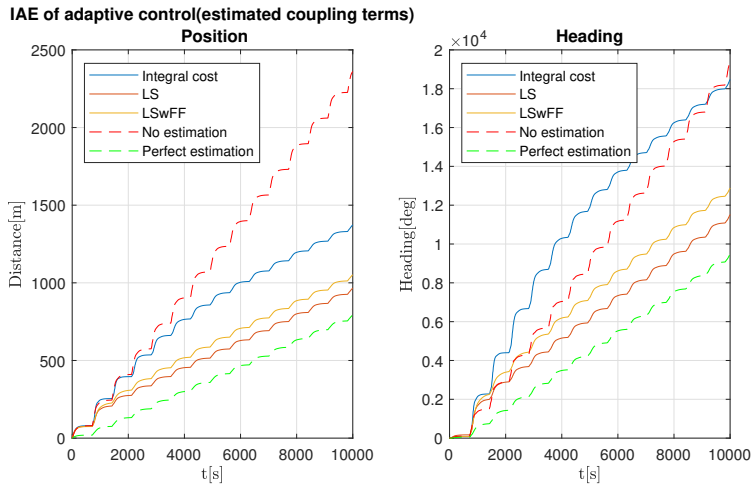

Figure 3.21: IAE of position and heading with ABC and estimated coupling terms

3.6 Discussion

With full PE it shows that it is possible to achieve full convergence of the estimated parameters to the model parameters. When keeping the coupling terms constant the convergence is relatively fast with accurate estimates in approximately 400 seconds. In this case the LS estimator outperforms the others with fastest convergence of all parameters. The biggest difference is shown in state d_{33} where the methods with forgetting factor diverges from the real value creating a big deviation before converging.

The complexity is increased when estimating the coupling terms as well, which is shown in the excess time before convergence. The different methods perform more similar with estimated coupling terms. Integral cost still has large deviations before converging with some parameters. The benefit of forgetting factor is shown in Figure 3.6. It seems like the minimum of the cost function does not correspond with the model parameter before the other parameters used in the estimations are sufficiently close to the real value. This results in a slow convergence with the LS method, as it does not forget the bad estimations in the beginning. Therefore without forgetting factor the estimator is less robust against changes.

When path following is introduced to simulate nominal operation the input signal is much less exited. This results in time periods where there is almost no update of the parameters, hence the convergence time is increased. With constant coupling terms the performance of the tested methods act similar as with full PE. LS is the quickest with all parameters converging around 800 seconds.

The simulations with path following and estimated coupling terms becomes very time consuming as the excitation of the input is reduced. With full PE all parameter estimations are sufficiently close after 1000 seconds, while with path following some parameters uses 4000-5000 seconds. The same trend as with full PE is shown as with path following. LS reaches good estimates of the real value quicker then the other methods, but struggles with the final convergence, with a small error in multiple parameters at 5000 seconds. Integral cost and LSwFF with forgetting factors struggles with bad estimates before 1000 seconds, where some of the estimations move further away than the initial guess. From that point the convergence rate is exponential, and surpasses the estimates from LS.

By implementing the estimations into the controllers it becomes an indirect adaptive controller. The distance error and heading error is taken into account. PIDwFF and PDwAFF both uses a feedforward term where the model estimates are updated. Both of these controllers struggle to improve the distance error, with the heading instability hard to neglect by updating the model. This is emphasised by the IAE plots of the distance error where no estimation and a perfect estimation of the model almost gives the same error. Comparing the heading error the parameter estimation improves the performance drastically for the controllers with feedforward. The slope of the IAE without estimation is approximately seven times higher than the controller using the exact model parameters. The overall performance comparing PIDwFF and PDwAFF is very similar which is expected as the adaptive term works as a more aggressive integral action. With the adaptive term it suppresses the error spikes more, but with fast oscillations in between trying to compensating for the model discrepancies.

ABC is the controller benefiting most from the parameter estimation. The IAE plots of both distance and heading with perfect estimation is approximately doubled compared to no parameter estimation. It manages to compensate the distance error from the heading instability better than the other controllers. This comes at the cost of a larger IAE in heading, as the perfect estimation still is worse than the other controllers without estimated parameters.

Table 3.9: IAE of distance at 10000 second

	Constant coupling terms			**Estimated coupling terms**		
Parameter	Integral cost	LS	LSwFF	Integral cost	LS	LSwFF
PIDwFF	3690	3714	3657	**3621**	3687	3706
PDwAFF	5022	4511	3976	**3838**	3964	4230
ABC	1124	**863**	1425	1373	966	1052

Table 3.10: IAE of heading at 10000 seconds

	Constant coupling terms			**Estimated coupling terms**		
Parameter	Integral cost	LS	LSwFF	Integral cost	LS	LSwFF
PIDwFF	2470	1542	3364	3448	**1527**	1805
PDwAFF	4853	2862	2742	2342	**1652**	2353
ABC	13957	**9169**	18905	18470	11519	12887

It is possible to estimate the coupling terms of the model parameters with the estimation methods tested. This results in a increased complexity and convergence time. The estimations with and without constant coupling terms is tested with controllers to see how it effects the performance and error. The distance error Table 3.9 and the heading error Table 3.10 in the IAE plots show the performance of the different estimation methods at 10000 seconds. The distance error of the methods is very close comparing PIDwFF and PDwAFF, while LS performs far better than the other methods when comparing the heading error.

From all of the IAE plots it becomes obvious that the best performing estimator is the LS method. With ABC it has quick convergence and can almost keep track of the perfect estimation. PIDwFF and PDwAFF is hard to separate when comparing the distance error, while with the IAE of the heading error LS is smallest in all case but one, where LSwFF barely beats LS. This is also evident in the parameter estimation plots as LS gives a close estimated of the model parameter very quick, without diverging much in the process. In comparison integral cost gives some very bad estimates before converging which results in the large IAE in some cases.

Chapter 4

Conclusion and future work

4.1 Conclusion

The introduced estimation methods manages to identify the parameters from the model of the ferry. When keeping the coupling terms of the model constant the convergence time is significantly faster than when the coupling terms are estimated. When estimating the parameters under nominal operations the excitation of the input is much lower giving large time periods where the parameters are not updated. It still manages to converge to the real model parameters with the little excitation, at the cost of increased convergence time. Even if it is not realistic for the ferry to operate in the same time horizon as in the simulations, the identification process can be saved and continued the next time the same amount of passengers is on board. This makes it possible to achieve better estimates over time, improving the control of the autonomous ferry.

The implementation of the Indirect adaptive controllers showed that it is possible to improve the controllers with more accurate model parameters. ABC improved both the positioning error and heading error substantially with an improved model, and PIDwFF and PDwAFF reduced the error of the heading. All of the estimation methods in the IAE plots eventually reached the same slope as when the exact model parameters were used in the controllers. LS stood out with the best convergence rate overall and reached the lowest IAE compared with the other methods in almost all cases.

4.2 Future work

Future work on this project could include:

- Implement the truster allocation algorithm which is used on the ferry. This will give more realistic simuations and the excitation of the input is more exact.
- Compare with direct adaptive control methods. Direct adaptive control does not estimate the parameters, but uses adaptive controller gains instead, to minimize the error. This could give good results with neglecting the instability in yaw of the ferry.
- Simulate changes in $\mathbf{D}$ depending on the number of passengers. Only model changes in the inertia matrix is tested. It is reasonable to assume that a different load will change the damping matrix as well. The damping matrix includes nonlinear terms and could create deviations between the models.
- Test the effect of noise and disturbances in the estimations. How evident will the Estimation drift be, and could this be compensated for.

Bibliography

Bitmead, R. R., 1984. Persistence of excitation conditions and the convergence of adaptive schemes. IEEE Transactions on Information Theory 30 (2), 183–191.

Fossen, T., 2011. Handbook of Marine Craft Hydrodynamics and Motion Control. John Wiley & Sons.

Ioannou, Sun, 1996. Robust adaptive control. Dover publications, Inc.

Jonas Linder, Martin Enqvist, T. I. F. T. A. J. F. G., 2015. Modeling for imu-based online estimation of a ship's mass and center of mass. IFAC-PapersOnLine 28 (16), 198–203.

OPONEO.CO.UK, 2016. Autonomy levels.
URL https://www.oponeo.co.uk/blog/what-europeans-actually-think-of-aut

Pedersen, A. A., 2019. Optimization based system identification for the milliampere ferry. Master's thesis, Norwegian University of Science and Technology, Trondheim, Norway.

SAEinternational, 2016. Levels of autonomy.

Sæther, B., 2019. Development and testing of navigation and motion control systems for milliampere. Master's thesis, Norwegian University of Science and Technology, Trondheim, Norway.

Weisstein, E. W., 2018. Fourier series–square wave.
URL http://mathworld.wolfram.com/FourierSeriesSquareWave.html

Zheng, J., 2019. Online identification method of nonlinear ship motion mathematical models from free-running tests. IEEE International Symposium on Industrial Electronics 2019-june (8781124), 1930–1936.

Zhu, M., H. A. W. Y.-Q. S. W.-Q., 2019. Optimized support vector regression algorithm-based modeling of ship dynamics. Applied Ocean Research 90 (101842).